NASA/CR–2015-218983

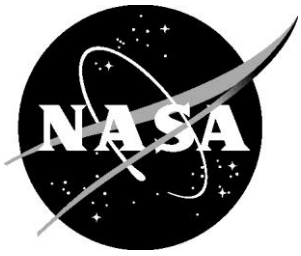

System-Level Experimental Validations for Supersonic Commercial Transport Aircraft Entering Service in the 2018-2020 Time Period

Phase II Final Report

Todd E. Magee, Spencer R. Fugal, and Lawrence E. Fink
Boeing Research and Technology, Huntington Beach, California

Eric E. Adamson and Stephen G. Shaw
Boeing Commercial Airplanes, Seattle, Washington

November 2015

NASA STI Program . . . in Profile

Since its founding, NASA has been dedicated to the advancement of aeronautics and space science. The NASA scientific and technical information (STI) program plays a key part in helping NASA maintain this important role.

The NASA STI program operates under the auspices of the Agency Chief Information Officer. It collects, organizes, provides for archiving, and disseminates NASA's STI. The NASA STI program provides access to the NTRS Registered and its public interface, the NASA Technical Reports Server, thus providing one of the largest collections of aeronautical and space science STI in the world. Results are published in both non-NASA channels and by NASA in the NASA STI Report Series, which includes the following report types:

- TECHNICAL PUBLICATION. Reports of completed research or a major significant phase of research that present the results of NASA Programs and include extensive data or theoretical analysis. Includes compilations of significant scientific and technical data and information deemed to be of continuing reference value. NASA counter-part of peer-reviewed formal professional papers but has less stringent limitations on manuscript length and extent of graphic presentations.

- TECHNICAL MEMORANDUM. Scientific and technical findings that are preliminary or of specialized interest, e.g., quick release reports, working papers, and bibliographies that contain minimal annotation. Does not contain extensive analysis.

- CONTRACTOR REPORT. Scientific and technical findings by NASA-sponsored contractors and grantees.

- CONFERENCE PUBLICATION. Collected papers from scientific and technical conferences, symposia, seminars, or other meetings sponsored or co-sponsored by NASA.

- SPECIAL PUBLICATION. Scientific, technical, or historical information from NASA programs, projects, and missions, often concerned with subjects having substantial public interest.

- TECHNICAL TRANSLATION. English-language translations of foreign scientific and technical material pertinent to NASA's mission.

Specialized services also include organizing and publishing research results, distributing specialized research announcements and feeds, providing information desk and personal search support, and enabling data exchange services.

For more information about the NASA STI program, see the following:

- Access the NASA STI program home page at http://www.sti.nasa.gov

- E-mail your question to help@sti.nasa.gov

- Phone the NASA STI Information Desk at 757-864-9658

- Write to:
  NASA STI Information Desk
  Mail Stop 148
  NASA Langley Research Center
  Hampton, VA 23681-2199

NASA/CR–2015-218983

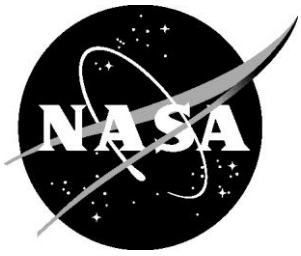

System-Level Experimental Validations for Supersonic Commercial Transport Aircraft Entering Service in the 2018-2020 Time Period

Phase II Final Report

Todd E. Magee, Spencer R. Fugal, and Lawrence E. Fink
Boeing Research and Technology, Huntington Beach, California

Eric E. Adamson and Stephen G. Shaw
Boeing Commercial Airplanes, Seattle, Washington

National Aeronautics and
Space Administration

Langley Research Center
Hampton, Virginia 23681-2199

Prepared for Langley Research Center
under Contract NNL10AA00T

November 2015

Available from:

NASA STI Program/Mail Stop 148
NASA Langlet Research Center
Hampton, Virginia 23681-2199
Fax: 757-864-6500

TABLE OF CONTENTS

1 EXECUTIVE SUMMARY

This report describes the work conducted under NASA funding for the Boeing N+2 Supersonic Experimental Validation project to experimentally validate the conceptual design of a supersonic airliner feasible for entry into service in the 2018 –to 2020 timeframe (NASA N+2 generation). The primary goal of the project was to develop a low-boom configuration optimized for minimum sonic boom signature (65 to 70 PLdB). This was a very aggressive goal that could be achieved only through integrated multidisciplinary optimization tools validated in relevant ground and, later, flight environments. The project was split into two phases. Phase I of the project covered the detailed aerodynamic design of a low boom airliner as well as the wind tunnel tests to validate that design (ref. 1). This report covers Phase II of the project, which continued the design methodology development of Phase I with a focus on the propulsion integration aspects as well as the testing involved to validate those designs.

One of the major airplane configuration features of the Boeing N+2 low boom design was the overwing nacelle. The location of the nacelle allowed for a minimal effect on the boom signature, however, it added a level of difficulty to designing an inlet with acceptable performance in the overwing flow field. Using the Phase I work as the starting point, the goals of the Phase 2 project were to design and verify inlet performance while maintaining a low-boom signature.

The Phase II project was successful in meeting all contract objectives. New modular nacelles were built for the larger Performance Model along with a propulsion rig with an electrically-actuated mass flow plug. Two new mounting struts were built for the smaller Boom Model, along with new nacelles. Propulsion integration testing was performed using an instrumented fan face and a mass flow plug, while boom signatures were measured using a wall-mounted pressure rail. A side study of testing in different wind tunnels was completed as a precursor to the selection of the facilities used for validation testing. As facility schedules allowed, the propulsion testing was done at the NASA Glenn Research Center (GRC) 8 x 6-Foot wind tunnel, while boom and force testing was done at the NASA Ames Research Center (ARC) 9 x 7-Foot wind tunnel. During boom testing, a live balance was used for gathering force data.

This report is broken down into nine sections. The first technical section (Section 2) covers the general scope of the Phase II activities, goals, a description of the design and testing efforts, and the project plan and schedule. Section 3 covers the details of the propulsion system concepts and design evolution. A series of short tests to evaluate the suitability of different wind tunnels for boom, propulsion, and force testing was also performed under the Phase 2 effort, with the results covered in Section 4. The propulsion integration testing is covered in Section 5 and the boom and force testing in Section 6. CFD comparisons and analyses are included in Section 7. Section 8 includes the conclusions and lessons learned.

2 SCOPE OF ACTIVITY

Overview

Since 1968, the Federal Aviation Administration (FAA) has banned civil supersonic flight over the continental United States (FAA Part 91.817) without a specific waiver. For all supersonic aircraft operating at the time, and in fact since then, the sonic boom produced as a result of flight at supersonic speeds has been deemed to be too annoying to the public at large to be declared acceptable. Limiting supersonic commercial aircraft to subsonic speeds over land has been a major obstacle to the development of second-generation commercial supersonic aircraft after the Concorde.

At the beginning of the 21st century, a renewal of interest in sonic boom research occurred, focusing on solving the problems that hinder the furtherance of a new generation of civil supersonic aviation. Since then, significant research has been conducted that shows it is possible to design a supersonic airplane with a very low sonic boom level by shaping the outer mold-line (OML). In August 2003, the first flight demonstration of this technology was successful in demonstrating that the sonic boom signature can be shaped by shaping the OML and that this signature-shaping persists to the ground. This flight experiment, called the Shaped Sonic Boom Demonstrator (SSBD), was a vital first step in validating the approach (ref. 2). Although the SSBD successfully demonstrated signature shaping on the front of an aircraft, it was readily apparent that to reduce the sonic boom noise, the entire aircraft and resultant sonic boom signature needed shaping. With advances in multidisciplinary optimization (MDO), complete aircraft shaping is now possible. Successfully implementing MDO, Boeing and others have developed the necessary techniques to design low-boom aircraft. The goal of this project was not only to conduct further low-boom concept designs using the latest techniques, but also to validate these methods in a wind tunnel environment.

2.1 Project Objectives and Goals

There are two main objectives for this project. The first objective is to validate the sonic boom and performance characteristics of an N+2-class supersonic vehicle specifically designed for low-boom operation. The second main objective is to assess the effect of nacelle and nozzle shaping on sonic boom levels and cruise performance for an N+2-class supersonic vehicle. The project is broken down into two distinct 18-month phases to address each of these objectives. The first phase of the project was designed to address the sonic boom and performance validation. The specific objectives for each phase are listed below.

Phase I objectives – Validate the low-boom configuration and its cruise efficiency.

- Starting with an N+2 supersonic vehicle, optimize the configuration to meet specified sonic boom and supersonic aerodynamic performance goals.
- Ensure that the low-boom concept sonic boom signature has front and aft signature shaping.
- Ensure that the low-boom concept has robust signature characteristics in under-track, off-track, and off-design flight conditions (i.e., Mach and CL).
- Validate the concept through sonic boom and supersonic performance wind-tunnel testing.

Phase II objectives – Assess the effect of nacelle and nozzle shaping on sonic boom and cruise performance.

- Starting with the Phase I supersonic vehicle, further optimize the configuration to meet sonic boom and cruise efficiency goals based on the lessons learned in Phase I testing.

- Focus on the effects of the inlet and plume on the sonic boom signature and supersonic cruise efficiency.
- Consider the interaction of the plume on aft signature shaping.
- Validate the new design through wind tunnel testing.

The table below illustrates the project aircraft performance goals, the most important of which is the 85-PLdB under-track sonic boom noise level with front and aft signature shaping. The second most important goal is the lift/drag (L/D) ratio remaining as good as the 765-076E configuration (i.e., L/D $\geq$7.0 at Mach = 1.6). In this study, Boeing chose to design the concept to the low end of the scale, with 35 passengers. The remaining goals are essentially fallouts of the previous three goals. Although aircraft design is not required to close in all disciplines, all disciplines (e.g., aerodynamics, stability and control, and mass properties) are to be assessed, and those that do not close are to be noted for future research.

N+2 Performance Goals

Objective	Goal
Sonic Boom (PLdB)	85 PLdB with front and aft shaping
Lift/Drag Ratio	As good as 765-076E
Cruise Speed	Mach 1.6–1.8
Range	4000 nmi
Payload (Passengers)	35 to 70
Fuel Efficiency (passenger miles per lb of fuel)	Fallout

2.2 Project Scope

This project employed a phased and gated approach to experimentally validate a supersonic N+2 low-boom concept. As discussed previously, the project was broken down into two 18-month phases. In Phase I a low-boom concept was developed. Once the concept was designed, its sonic boom and performance was assessed using high-fidelity CFD. The results of this assessment were presented at a gate review with NASA and the concept was approved to move forward with fabrication and testing. Two wind-tunnel models were fabricated, two versions of sonic boom models and a performance wind-tunnel model, which were tested at the NASA ARC 9 x 7-Foot Wind Tunnel.

The scope of Phase II essentially mirrored the Phase I effort, except that the focus was on the propulsion integration effects and the effect of the inlet and nozzle plume on the sonic boom and the aircraft aerodynamic performance. The low-boom concept for Phase II was updated based on lessons learned in Phase I. Additional design work was conducted that leveraged nacelle and nozzle shaping with aircraft integration to achieve low sonic boom noise and high installed propulsion efficiency. The design passed a gate review similar to the one conducted in Phase I. After passing this gate review, wind tunnel models and parts were fabricated for the sonic boom model and the cruise performance model. Upon completion of the wind tunnel models, the propulsion and boom wind tunnel tests were conducted. Results from the tests were compared against CFD for validation and documented.

2.3 Project Plan and Schedule

The project plan was organized by Work Breakdown Structure (WBS), with each phase having a similar set of items. The Phase I project plan is listed below.

Phase I

3.1 Development of Generation 3.0 Geometry (American Recovery and Reinvestment Act (ARRA)-funded task).
3.1.1 Develop the low-boom concept
3.1.2 Assess low-boom concept and preliminary model mount system.
3.1.3 Gate Review 1.
3.2 Fabrication of Experimental Validation Hardware (ARRA-funded task).
3.3 Evaluation of Existing NASA Sonic Boom Pressure Rails (ARRA-funded task).
3.4 Validation Analysis.
3.5 Test Planning, Pretest Support, and Post-test Support.
3.6 Wind Tunnel Test Support.
3.7 Technical Management, Planning, and Deliverables.
3.7.1 ARRA-funded tasks.
3.7.2 NASA-funded tasks (Gate Review 2 is included in this WBS item).

In Phase I, ARRA-funded activities include WBS items 3.1, 3.2, 3.3, and 3.7.1. The remaining WBS items were NASA-funded activities.

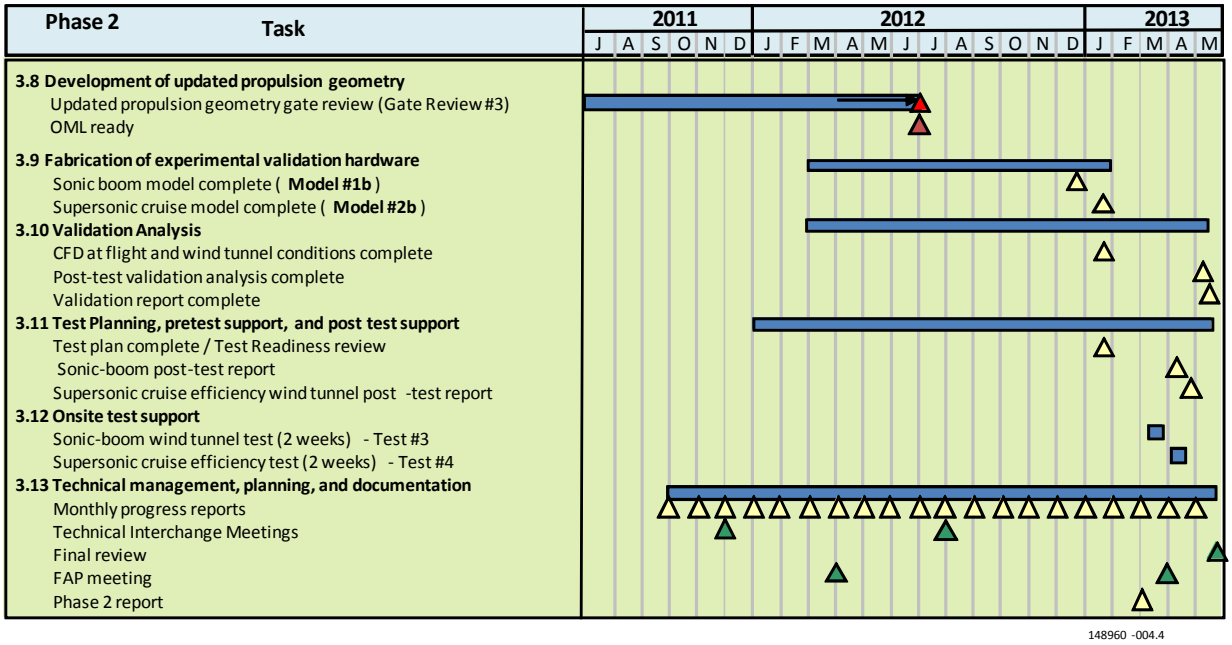

Figure 2-1. Phase II project schedule.

The Phase II project plan is listed below:

Phase II

3.8 Development of Updated Propulsion Effects Geometry - Gate Review 3.
3.9 Fabrication of Experimental Validation Hardware.
3.10 Validation Analysis.
3.11 Test Planning, Pre-test Support, and Post-test Support.
3.12 Wind Tunnel Test Support.
3.13 Technical Management, Planning, and Documentation.

All WBS elements in Phase II are NASA-funded activities.

From the project plan, an integrated master schedule was developed (Figure 2.1). An additional task was added during Phase II, which was to do a short study on the feasibility of wind- tunnel testing at different NASA facilities that would cover the range of conditions required for propulsion and boom testing. This task consisted of short tests at the NASA GRC 8 x 6-Foot and NASA ARC 11-Foot Wind Tunnels, and the results from these tests were used to make a facility recommendation for the validation test.

2.4 Project Organization

Figure 2.2 shows the project organization. NASA leadership for the project consisted of Peter Coen (NASA Supersonics Project manager) and Linda Bangert (N+2 Experimental Validation contracting officer's technical representative [COTR]). The project principal investigator was Todd Magee, and the project co-investigator is Eric Adamson. Personnel from both Boeing Research & Technology and Boeing Commercial Airplanes were involved in the project. A single supplier, Tri Models Inc., was selected for wind-tunnel model fabrication. Boeing functional leadership and technical contributors also are identified in Figure 2.2.

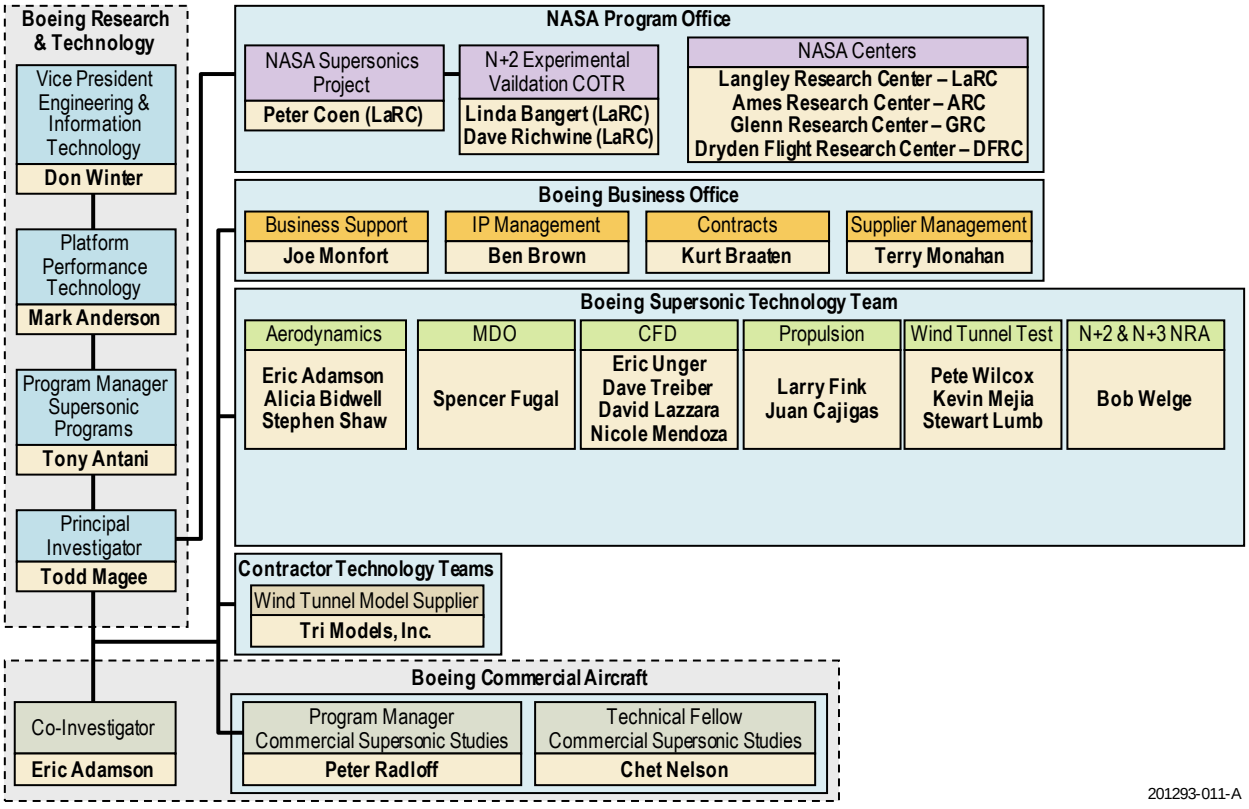

Figure 2-2. Phase II project organization.

2.5 Project Deliverables

Phase II of the N+2 project deliverables are shown in Figure 2.3.

The remainder of this report focuses specifically on the Phase II part of the project. The Phase I information in this section was provided as background. The Phase I report is listed as a reference.

#	Period	Deliverable	Due Date (Months after Contract Award
28	Phase 2	CAD definition for OML that addresses the influence of the inlet and plume on the sonic boom signature and cruise performance	24
29	Phase 2	Sonic boom wind tunnel model (Model #1b)	29
30	Phase 2	Required support hardware for Model #1b	29
31	Phase 2	Model #1b documentation (drawings, stress report, quality report)	29
32	Phase 2	Model #1b support hardware documentation	29
33	Phase 2	Supersonic cruise efficiency model (Model #2b)	30
34	Phase 2	Required support hardware for Model #2b	30
35	Phase 2	Model #2b documentation (drawings, stress report, quality report)	30
36	Phase 2	Model #2b support hardware documentation	30
37	Phase 2	Phase 2 validation report	35
38	Phase 2	Sonic boom wind tunnel test plan – Test #3	30
39	Phase 2	Sonic boom wind tunnel test report – Test #3	32
40	Phase 2	Supersonic performance wind tunnel test plan – Test #4	30
41	Phase 2	Supersonic performance wind tunnel test report – Test #4	33
42	Phase 2	Phase 2 final report	35
43	Phase 2	Quarterly progress reports	21, 24, 27, 30, 33
44	Phase 2	2011 and 2012 FAP Annual Meeting PowerPoint presentations	22, 34
45	Phase 2	Gate Review #3 briefing	24
46	Phase 2	Technical Interchange meeting briefings	20, 28
47	Phase 2	Phase 2 review briefing	35

Figure 2-3. Phase II deliverables.

3 PROPULSION SYSTEM CONCEPT DEVELOPMENT

The Phase II propulsion system design and development effort continued the Phase I effort with special attention on the effect of the inlet and plume on the sonic boom signature and supersonic cruise efficiency. Phase I results showed that with the overwing engine installation, the sonic boom characteristics of the chosen configuration were relatively insensitive to the propulsion system integration. The Phase II effort was aimed at improving the operating efficiency of the engine while maintaining an acceptable sonic boom signature.

3.1 Nacelle Installation Study

The initial part of Phase II was spent investigating the best overwing propulsion installation configuration. Figure 3-1 shows some different installation concepts that varied inlet type, location, and duct length.

Configuration 1 used a nacelle that was most similar to the Phase I QEVC design, which had shown some level of acceptable performance. The nacelle was moved so the nozzle was two diameters forward of the aft-deck trailing edge. The inlet had a translating cowl for low-speed operation and a bump type inlet. The potential disadvantages of this configuration would be the boundary layer ingestion of the bump inlet, strake vortex ingestion, and power induced control effects.

Configuration 2 had an aft body mounted nacelle with a 2-D external compression inlet. In this position, the inlet would have a 3-D diverter. The inlet had a translating cowl for low-speed operation. The potential advantages of this configuration were less chance for strake vortex ingestion and the opportunity to derive a more blended arrangement with potential weight and drag savings. The disadvantages were safety concerns due to rotor burst and egress, and power induced control effects.

Configuration 3 had a body mounted long duct nacelle with a waverider type inlet. The inlet would have a translating cowl for low-speed operation. For this nacelle, the potential advantages included the fact that the strake and inlet could be optimized as a unit, there was ample duct length to mitigate distortion ingestion, and the opportunity to derive a more blended arrangement. The potential disadvantages included safety (rotor burst, egress), potentially higher fuel consumption (SFC), power induced control effects, and passenger acceptance due to a lack of windows.

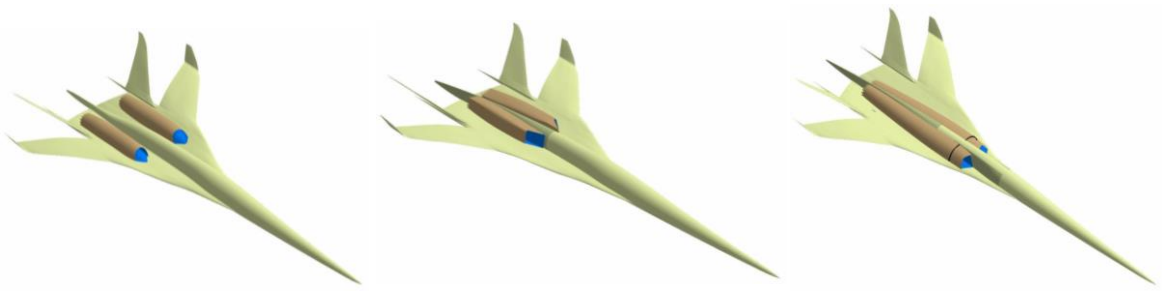

Configuration 1	Configuration 2	Configuration 3
• Baseline Nacelles in forward location • Bump Inlet	• Notional Aft Body Mounted Nacelles • 2-D external compression Inlet	• Notional Body Mounted Long Duct Nacelle • “Waverider” Inlet

Figure 3-1. Nacelle installation concepts.

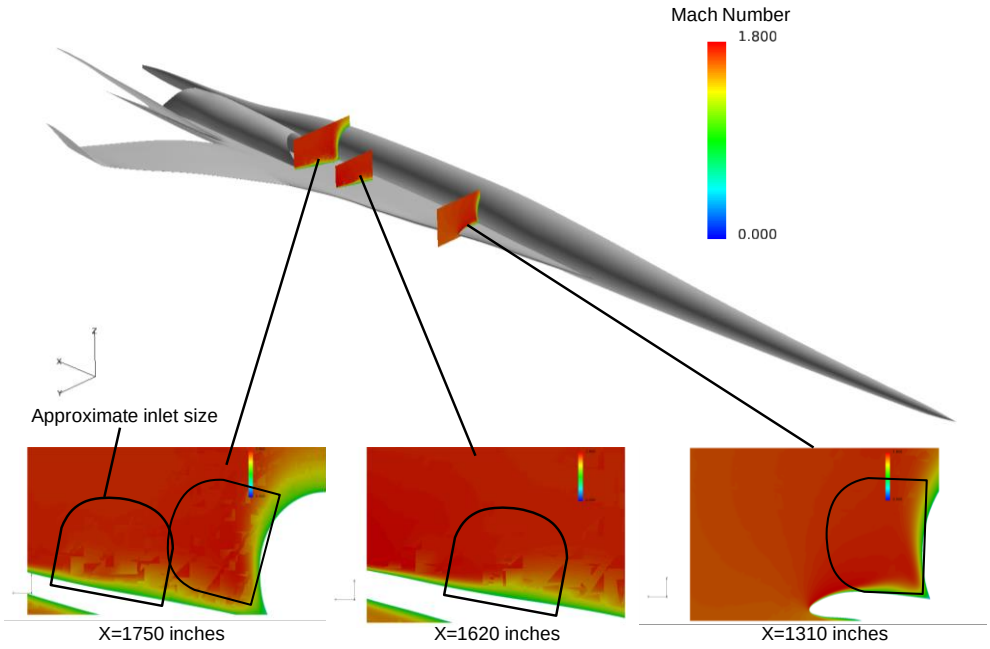

Figure 3-2. Inlet flowfield survey, Mach 1.6, alpha=6 degrees.

An inlet flow field survey was conducted using CFD (OVERFLOW) in order to characterize the inlet conditions for the potential engine installation configurations. Figures 3-2 and 3-3 show the results for Mach 1.6 at two angles of attack. It was found that inviscid flow analysis showed little variation in all quantities between design variations, necessitating the use of viscous analysis.

The conclusion of the inlet study was to select the forward mounted wing installation (Config 1) as it allows the greatest potential for community noise reduction with a minimum amount of drag penalty.

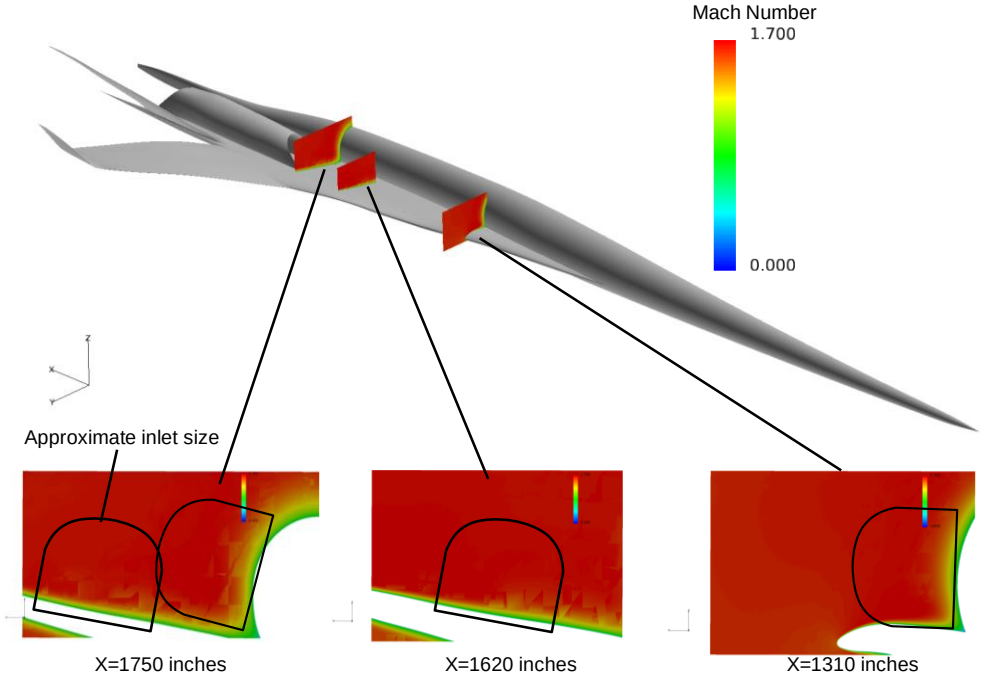

Figure 3-3. Inlet flowfield survey, Mach 1.6, alpha=3 degrees.

3.2 Inlet and Nozzle Design

Two types of inlets were used as starting points for the inlet design effort: the elliptical cowl ramp inlet (ECRI) and the the elliptical cowl cone inlet (ECCI). The ECRI inlet had a 2-D type external compression ramp, while the ECCI had a cone.

The design effort for the ECRI inlet involved a Design of Experiments optimization using OVERFLOW with a D-Optimal design selector. Initially, 13 isolated inlets were developed with the following six design variables: cowl ellipse ratio, engine height (offset of engine center relative to inlet ramp leading edge), engine station (relative to ramp leading edge), inlet width, design throat Mach, and sidewall divergence angle (Figure 3-4). The results from these 13 cases were then used to develop 49 cases, using a Latin Square design selector, for the same study variables. Each of these cases were run in an isolated configuration with the inlet conditions representative of the flowfield above a wing, and also an installed configuration. Eventually, an additional six inlets were added to the group. For the 55 different inlets, the following geometric variations were used:

- Inlet ellipse ratio varied from 1.0 to 2.0
- Engine height varied from 27.5 to 32.5 inches
- Mach at the throat varied from 1.1 to 1.2
- Engine station varied from 253 to 279 inches
- Inlet width varied from 55 to 75 inches

For each isolated CFD run, the following conditions were used:

- Inlet Mach = 1.66
- Unit Reynolds number = 181,697/inch
- Back pressure varied from P/Oinf = 3.98 to 4.02 by 0.01 (5 cases per geometry). The back pressure resulting with the highest recovery was used.

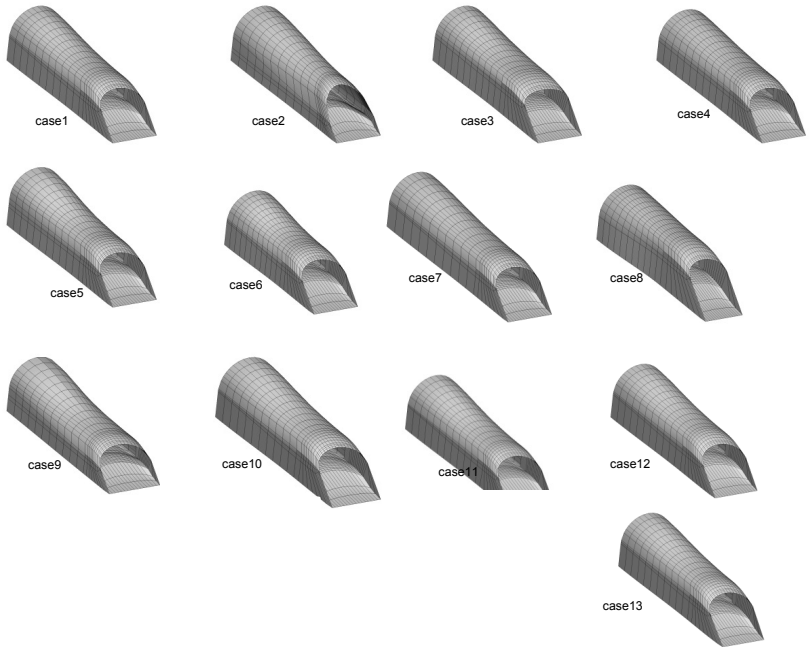

Figure 3-4. Initial 13 ECRI parametric inlet concepts.

The best performing inlet from the 55 was selected for additional cycles of detailed optimization. The final configuration, the ECRI52-9013 was analyzed to show a significant improvement over a conventional 2-D inlet.

The initial performance assessments for the ECCI (Figure 3-5) indicated that they would need more time and effort to achieve a good design than an ECRI type inlet, so the concept was dropped in favor of the ECRI.

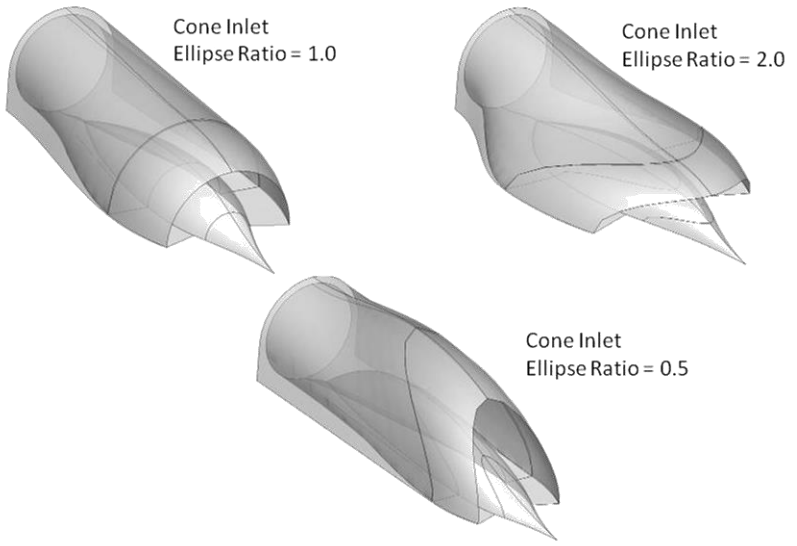

Figure 3-5. ECCI inlet concepts.

A parametric nozzle design effort similar to the inlet design was conducted (Figure 3-6). The nominal nozzle was D-shaped with geometric variation for convergence and divergence, scarf angle, throat/engine width, and nozzle length.

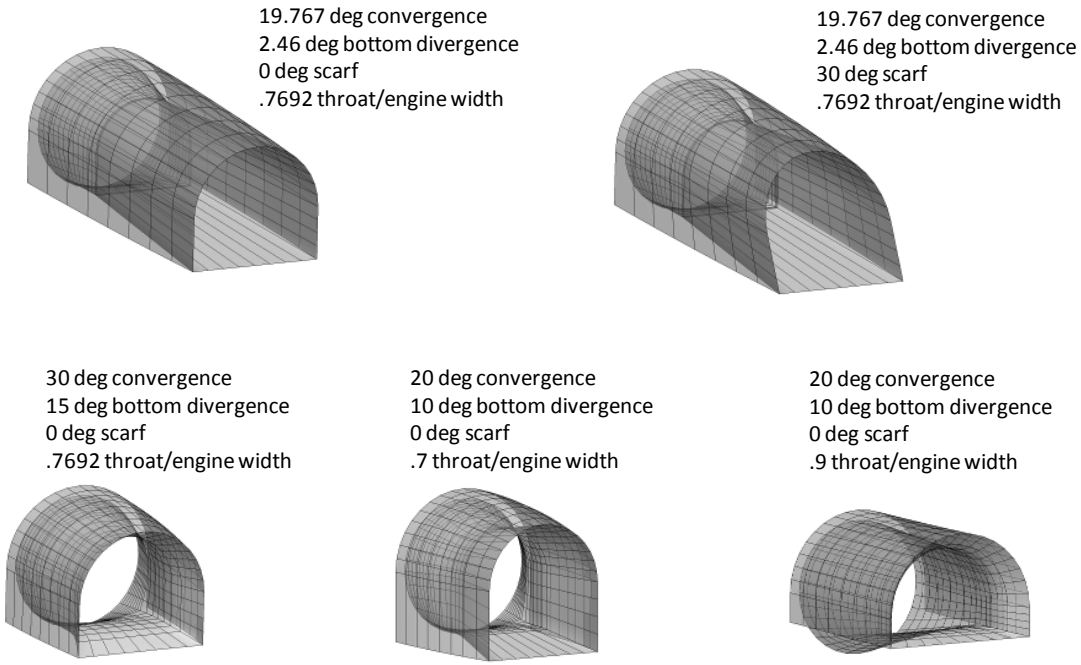

Figure 3-6. Nozzle concepts.

The final inlet and nozzle design was selected to provide the optimum balance between high pressure recovery, low distortion, and low drag. The inlet/nozzle combination selected had the following geometric parameters:

- Expansion ratio 1.459
- Engine height 27.5 inches
- Throat Mach 1.158
- Engine station 279.6 inches
- Inlet width 60.1 inches
- Inlet recovery 97.3%
- Inlet distortion 3.9%
- AIP Mach 0.446
- Inlet mass flow ratio 0.9546
- Drag 0.00118

4 EXPLORATORY TESTING

Under Phase I, the NASA ARC 9 x 7-Foot Wind Tunnel was selected for all experimental validation testing. The selection was based on the facility's large cross-section and availability. However, there was some conflicting data available as to the facility's flow quality: while the 1990's HSR tests and a 2008 NASA/Gulfstream sonic boom test indicated flow non-uniformity and time-dependent uncertainty, results from a 1971 sonic boom test showed accurate data was obtained out to significantly large separation distances (~86 inches; though any corrections or smoothing of the data were not documented). During Phase I testing, the spatial and time dependent uncertainties were shown to be significant, to the extent that without adjusting the test techniques (running large position sweeps and averaging the results) acceptable data would not be possible. With the emphasis of the Phase 2 Validation effort on propulsion integration, and the need to more completely characterize inlet performance over transonic and supersonic speeds, the NASA ARC 9 x 7-Foot Wind Tunnel was insufficient by itself since it is supersonic only. A series of short tests was therefore proposed at different wind tunnel facilities that would be able to provide an expanded Mach range to cover these off-design conditions. The NASA ARC 11-Foot Wind Tunnel and the NASA GRC 8 x 6-Foot Wind Tunnel were proposed, with the NASA ARC 11-Foot Wind Tunnel being considered as the complementary transonic facility to the NASA ARC 9 x 7-Foot supersonic wind tunnel. As exploratory tests with a short entry (less than 1 week) and with a short preparation time (a few months), the goal was to minimize the cost and effort needed to incorporate the model hardware and pressure rail instrumentation into each tunnel while ensuring that the tested configurations would be able to provide a definitive answer as to the quality of the data gathered. Additionally, these facilities would be evaluated in terms of productivity. The results of these short tests would be used to form a recommendation as to which facility to use for the final validation test. A short comparison of the characteristics of these three tunnels is provided here.

Wind-Tunnel Characteristics

	Ames 11-Foot*	Ames 9 x 7-Foot*	Glenn 8 x 6-Foot**
Test Section	11- by 11-Foot Slotted Walls	9- by 7-Foot Solid Walls	8- by 6-Foot Perforated Walls (transonic section)
Tunnel circuit	Closed circuit	Closed circuit	Closed circuit***
Mach Range	0.2 – 1.5	1.54 – 2.56	0.36 – 2.0

*Test Planning Guide for High-Speed Wind Tunnels, Ames Research Center
**NASA Lewis 8- by 6-Foot Supersonic Wind Tunnel User Manual
***vented to atmospheric

4.1 NASA GRC 8 x 6-Foot Wind Tunnel Exploratory Test

Test Objectives and Scope

The objectives for the exploratory test were to:

- Gather pressure rail data at the NASA GRC 8 x 6-Foot Wind Tunnel using several existing models
- Quantify the temporal and spatial uncertainties of the 8 x 6-Foot Wind Tunnel
- Gather force and moment data; evaluate the effects of temperature on the balance
- Evaluate the capability of the 8 x 6-Foot Wind Tunnel to measure small differences in the boom signal due to propulsion integration effects

- Develop and understand the productivity differences between the NASA GRC 8 x 6-Foot, NASA ARC 9 x 7-Foot, and NASA ARC 11- by 11-Foot Wind Tunnels
- Quantify the "unknown unknowns" of boom testing at the NASA GRC 8 x 6-Foot Wind Tunnel
- Calibrate CFD tools estimates

The focus of the NASA GRC exploratory test was to gather boom data and also check the functionality of the balance at the elevated 8 x 6-Foot test section temperatures—at times, the operating temperatures were above 180° F. It was felt that being able to complete these items successfully would cover any issues that could come up for future propulsion testing. The 14-inch pressure rail was used as the baseline pressure instrumentation, however, there was interest by NASA to also install the 2-inch pressure rail. Some additional occupancy time was allotted for the 2-inch pressure rail installation and a limited set of data runs.

Test Calendar

The following figures show the test calendar for the NASA GRC 8 x 6-Foot exploratory test:

	Shift Hour							
	1	**2**	**3**	**4**	**5**	**6**	**7**	**8**
Monday (Labor Day Holiday)								
Shift 1 Tuesday 9-4-13	Performance Model	Performance Model	Performance Model	Out of dry air				
Shift 2 Wednesday 9-5-13	Facility Startup	Performance Model	Performance Model	Performance Model	Performance Model force polars			
Shift 3 Thursday 9-6-13	Facility Startup	Boom Model	Out of dry air					
Shift 4 Friday 9-7-13	Facility Startup	Boom Model	Boom Model	Model Change	BOR AS2	Out of dry air		

Figure 4-1. NASA GRC 8 x 6-Foot Wind Tunnel exploratory test calendar, Week 1.

	Shift Hour							
	1	2	3	4	5	6	7	8
Shift 5 Monday 9-10-13 (No Testing)								
Shift 6 Tuesday 9-11-13	Facility Startup	BOR AS2	BOR AS2	BOR AS2	Model Change	Model Change	Cone	Out of dry air
Shift 7 Wednesday 9-12-13	Boom Model	Boom Model	Model Change	Boom Model	Boom Model	Boom Model	Out of dry air	
Shift 8 Thursday 9-13-13	Model Change	Boom Model 2 inch rail	Boom Model 2 inch rail	Boom Model 2 inch rail	Boom Model 2 inch rail	Boom Model 2 inch rail	Out of dry air	
Shift 9 Friday 9-14-13	BOR AS2 2 inch rail	BOR AS2 2 inch rail	Model Change	Cone 2 inch rail	Cone 2 inch rail			

Figure 4-2. NASA GRC 8 x 6-Foot exploratory test calendar, Week 2.

Test Hardware

The NASA GRC exploratory test made use of existing models and pressure rail instrumentation. The larger performance model was used for boom and force testing, while the smaller boom model was used for boom testing at larger separation distances from the rail. The AS2 body of revolution model was also tested as a reference, as well as the 8-degree cone. Both the 14-inch pressure rail and the 2-inch pressure rail were used during the test.

The support hardware consisted of the linear actuator and the SR-229 sting. The linear actuator was mounted to the facility pitch/traverse strut. The installation was inverted, i.e., the pressure rail was mounted to the ceiling and the model was run inverted (Figure 4-3). This was necessary since the ceiling plates offered the best options in terms of modifications for placement and mounting the pressure rail hardware. The model and rail were placed in the transonic test section and where the model could be imaged with the schlieren system through the windows. A roll mechanism was not used for the exploratory test.

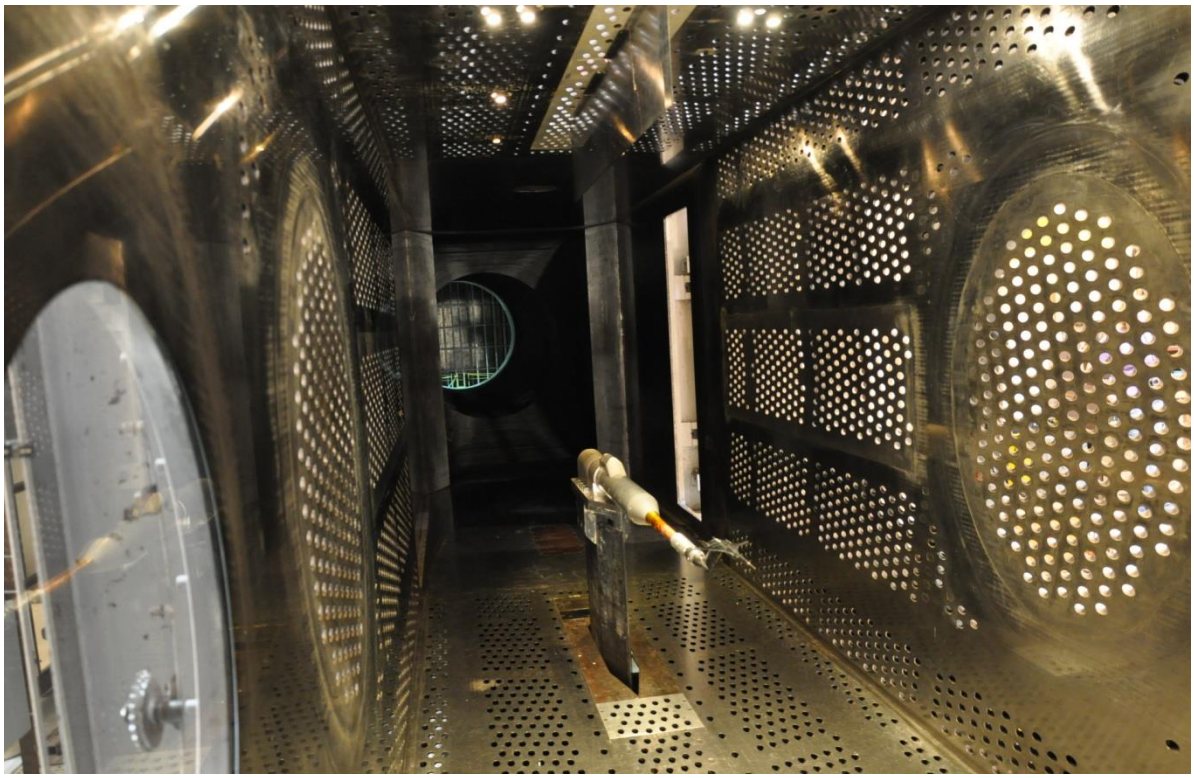

Figure 4-3. BM (Boom Model) at the NASA GRC 8 x 6-Foot Wind Tunnel.

Test Results

The majority of the test time during the NASA GRC exploratory entry was spent fine tuning the process for producing good sonic boom data. The boom data collection methods that were initially used had been developed at the NASA ARC 9 x 7-Foot Wind Tunnel and provided a starting point for data collection at the NASA GRC 8 x 6-Foot Wind Tunnel. These methods covered data acquisition and data settling times, up-and-away reference runs, and using the average of multiple signals to offset the effects of temporal and spatial variations in the tunnel. During the first week it was found that the boom data collected was unsatisfactory and the tunnel productivity was worse than anticipated. During the second week of testing, the data collection methods continued to be refined and by the end of the test, the boom data quality was generally satisfactory even for the smaller boom model at the further distances from the pressure rail. Wind tunnel productivity was improved only slightly, but was primarily a function of the ambient weather. Figures 4.4 – 4.7 show results that incorporate all (or most) of the lessons learned during the exploratory test.

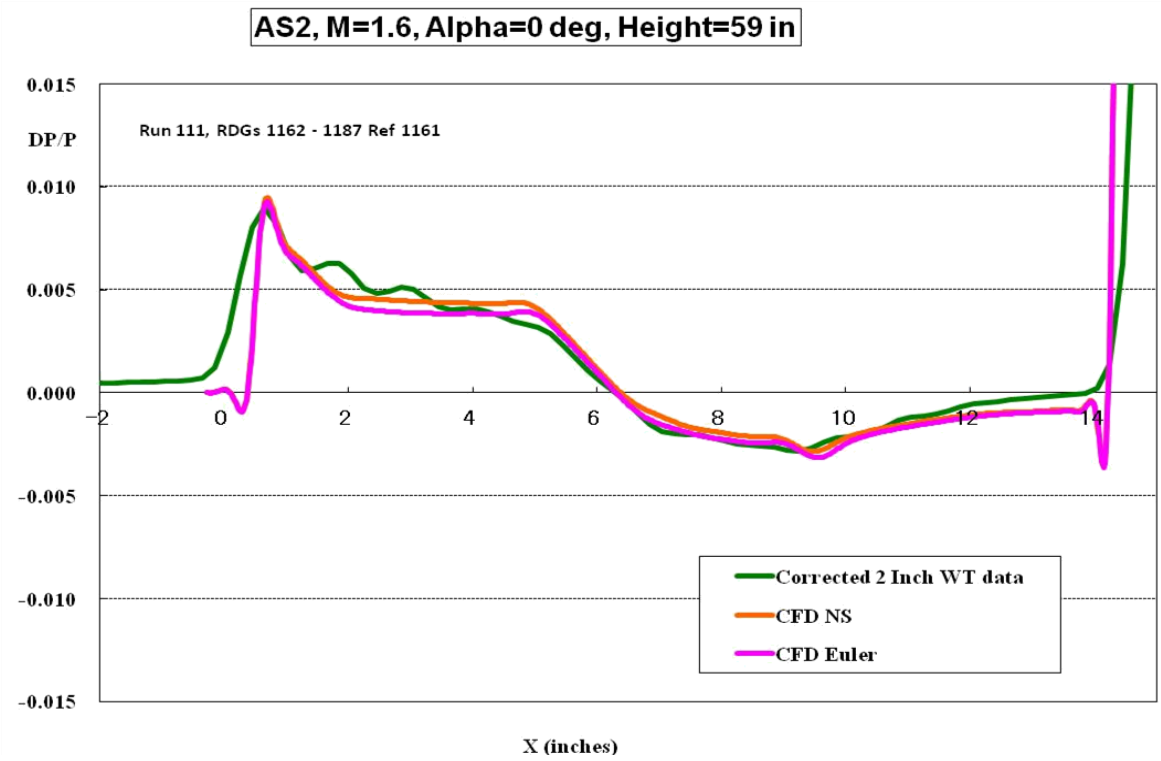

Figure 4-4. NASA GRC exploratory test results, AS2.

Figure 4-4 shows the results for the AS2 body of revolution compared to CFD from the 2-inch rail The rail data has been corrected for first order tare and interference effects such as wind tunnel boundary layer and solid wall pressure reflections. Additional details cannot be provided as the correction method is proprietary. The wind-tunnel data shows a less than sharp initial nose shock followed by some slight oscillations where the CFD shows a flat-top signature. The CFD and wind tunnel have fairly good agreement on the aft part of the model.

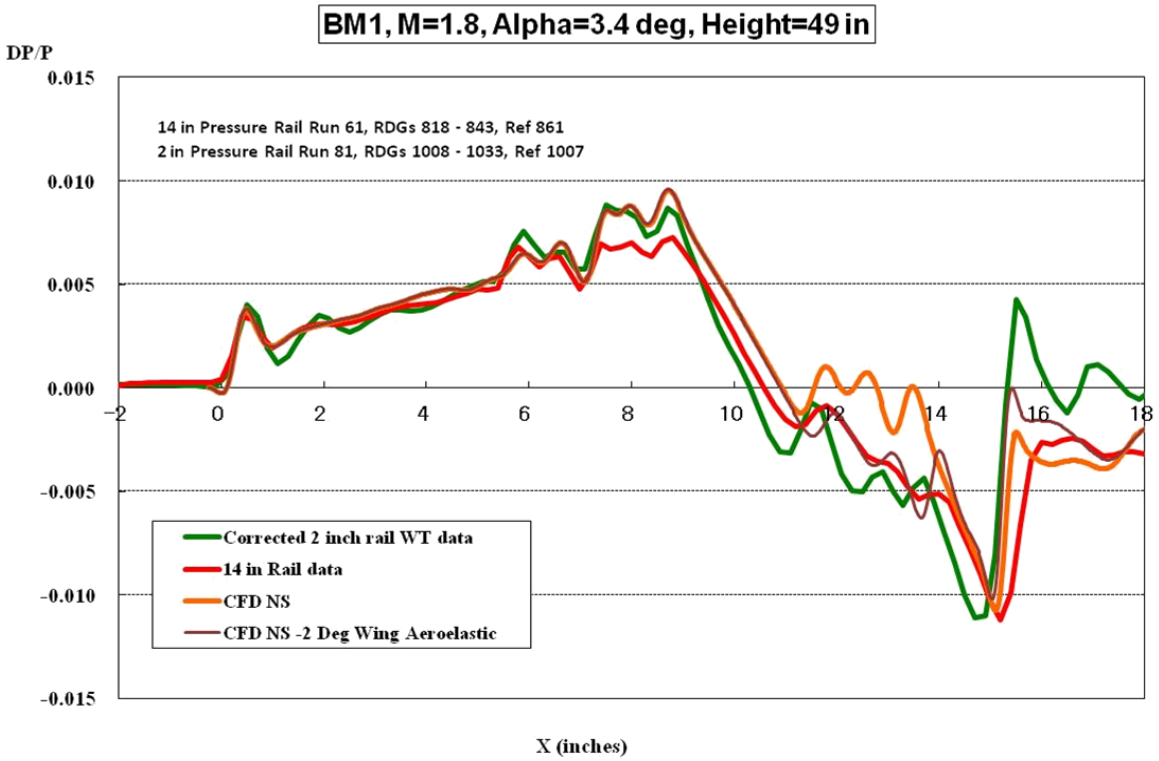

Figure 4-5. NASA GRC 8 x 6-Foot BM model results.

Figure 4-5 shows the results for the BM model compared to CFD for both the 14-inch and 2-inch rail The rail data has been corrected for first order tare and interference effects such as wind tunnel boundary layer and solid wall pressure reflections. Additional details cannot be provided as the correction method is proprietary. An additional CFD run with an assumed aeroelastic effect of 2° of washout is also shown. The wind tunnel data shows good agreement with the nose shock shape. The 2-inch rail data shows some slight oscillations aft of the nose shock, whereas the 14-inch rail data is a bit low at the signal peaks at the mid-body location. There is a significant difference at the aft-body (nacelle/wing) location, however, the CFD with the washout correction pushes the signal in the right direction.

Lessons Learned and Conclusions

Several methods of operating the wind tunnel were developed and implemented during the course of the test that improved the data quality. The usual process for z-sweeps and up-and-away reference runs is to pause a certain increment of time for data settling. However, in the 8 x 6-Foot Wind Tunnel, the support strut is not continuous from the floor to the ceiling. Thus, any small amount of model height or alpha change (the center of rotation is underneath the floor) causes a blockage change and a resulting Mach number change. While the tunnel has an automated system for getting back on condition within a tolerance, it was not quick enough. Two solutions were devised:

- Allow extra time for the tunnel to return within the specified Mach tolerance. Additionally, the tunnel operator can dial in the Mach number to a tighter tolerance.
- Use the linear actuator where the most retracted position is the reference position, and the most extended positions are the data positions. For this option the strut does not move, minimizing any blockage changes. This method only applies to the smaller boom models.

While option 1 would allow the test to proceed using the typical method of up-and-away reference runs or z-sweeps, the time penalty to allow the tunnel control system to maintain Mach number was not acceptable. Option 2 was selected as the preferred method for developing the process for gathering quality boom data. In addition to limiting the Mach variation by using the linear actuator, the Mach number tolerance was further tightened from the nominal +/-0.002 to +/-0.001.

Another major lesson learned during the NASA GRC exploratory test was the effect of the ambient weather conditions on the tunnel productivity. While the 8 x 6-Foot Wind Tunnel is a closed circuit wind tunnel, it continuously draws in air from the outside through the plenum evacuation system during supersonic testing. Air drawn in is passed through the dessicant beds, and as soon as the beds are saturated, the dewpoint in the wind-tunnel circuit rises rapidly to the point where fog can be seen in the test section. Unfortunately, during the exploratory test window, Cleveland experienced the remnants of a tropical storm, and atmospheric conditions were unfavorable for sustained supersonic testing. The capability of the dessicant beds to provide dry air during testing are a function of temperature and humidity, and is illustrated in Figure 4-6. The temperature during the exploratory test was about 65-70° with 80-90 percent humidity and resulted in, at most, a few hours of dry air per shift, as can be seen in the test calendar.

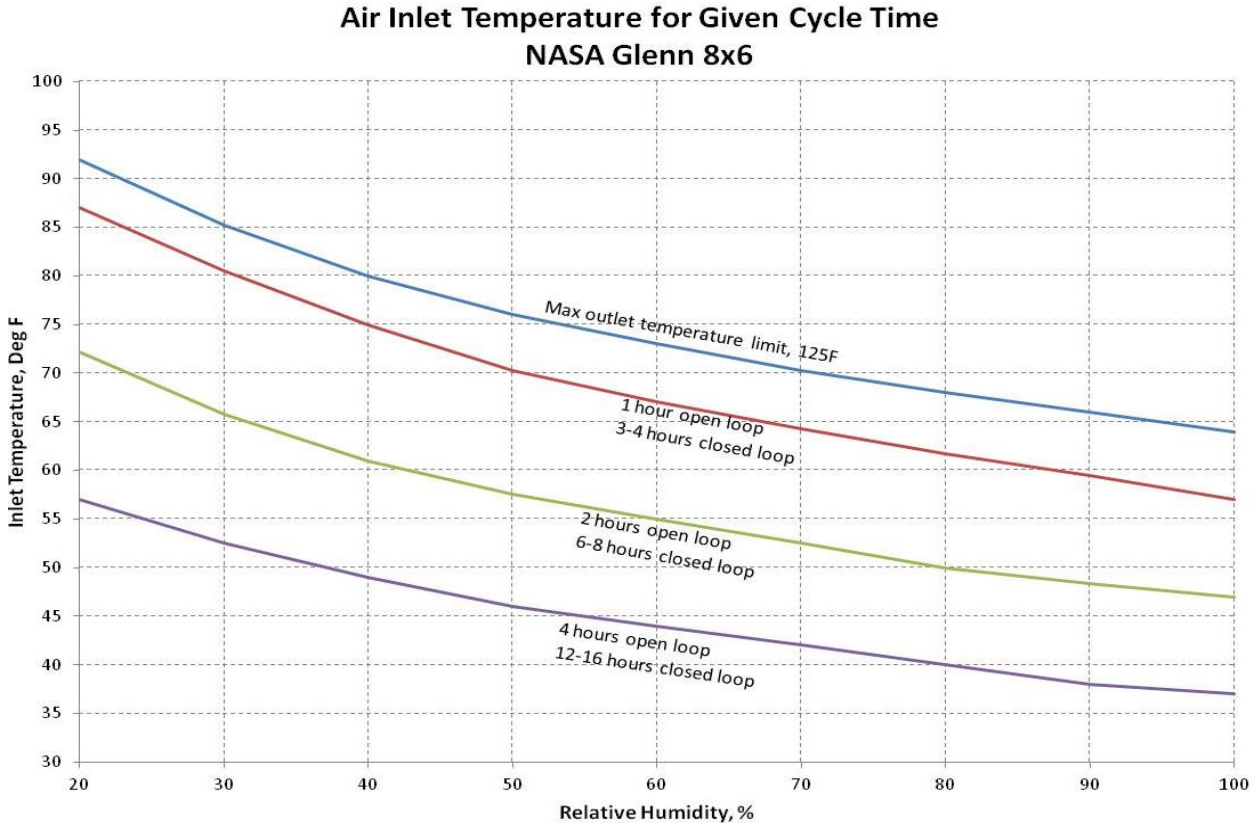

Figure 4-6. NASA GRC 8 x 6-Foot dry air estimation.

Temperature effects on the balance data were also of concern at the NASA GRC 8 x 6-Foot Wind Tunnel due to the elevated temperatures in the test section (as high as 180°F at Mach 1.8). Several drag polars were taken and the results seem to show that there were no apparent effects due to test section temperatures.

The conclusions derived from the NASA GRC exploratory test were that the tunnel can produce boom data of at least the same quality as the NASA ARC 9 x 7-Foot Wind Tunnel, if not better. However, there is a potential limitation on productivity due to the availability of dry air, which is a function of ambient temperature and humidity. Figure 4-7 shows the average temperatures and humidity at Cleveland International Airport, which suggest running a test during the colder parts of the year in order to have enough dry air to cover the planned testing hours per day. The NASA GRC 8 x 6-Foot Wind Tunnel also offers an advantage of being able to cover the desired subsonic and supersonic Mach range in a single facility.

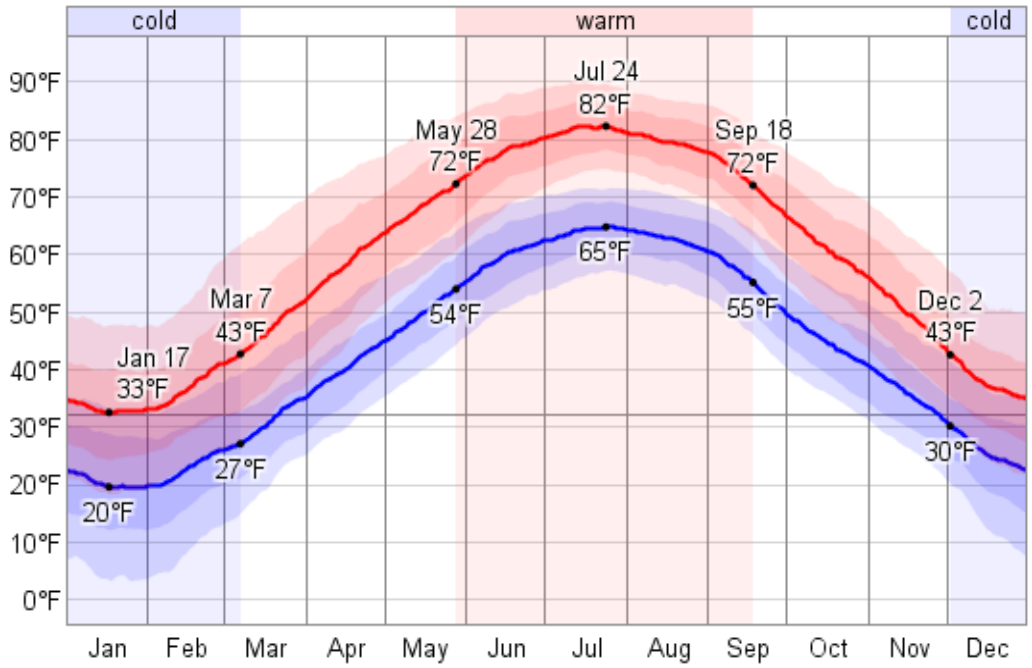

Figure 4-7. The average temperature at Cleveland International Airport (weatherspark.com).

4.2 NASA ARC 11-Foot Exploratory Test

Test Objectives and Scope

The objectives of the exploratory test were to:

- Gather pressure rail data at the NASA ARC 11-Foot Wind Tunnel using several existing models
- Quantify the temporal and spatial uncertainty of the NASA ARC 11-Foot Wind Tunnel
- Gather force and moment data
- Evaluate the capability of the NASA ARC 11-Foot Wind Tunnel to measure small differences in the boom signal due to propulsion integration effects
- Determine the maximum attainable Mach number for the N+2 model installation

- Develop and understand the productivity differences between the NASA GRC 8 x 6-Foot, NASA ARC 9 x 7-Foot, and NASA ARC 11-Foot Wind Tunnels
- Quantify the "unknown unknowns" of boom testing at the NASA ARC 11-Foot Wind Tunnel
- Calibrate CFD tools

The NASA ARC 11-Foot Wind Tunnel was selected for an exploratory test to see if it could be successfully used as a complementary facility to the NASA ARC 9 x 7-Foot Wind Tunnel to cover the desired Mach range. The published Mach capabilities of the wind tunnels indicate at least some gap between the maximum Mach of the 11-Foot Wind Tunnel and the minimum speed of the 9 x 7-Foot Wind Tunnel, however, the actual maximum Mach number attainable with the model installed would be determined during the test. Gathering force data at the Ames facility was somewhat of a second priority item since temperature effects at the NASA ARC 11-Foot were not seen as an issue, and would be similar to the 9 x 7-Foot Wind Tunnel.

Test Calendar

The following figures show the test calendar for the NASA ARC 11-Foot Wind Tunnel exploratory test:

	Shift Hour								
	1	2	3	4	5	6	7	8	9
Shift 1 Friday 6-1-13	Install	Install	Install	Install	Install	Install	Install	Install	
Shift 2 Monday 6-4-13	Install	Install	Install	install	Install	Install	Install	Install	
Shift 3 Tuesday 6-5-13	Install	Install	Install	Warmup/ Conditioning	Warmup/ Conditioning	Troubleshooting	Troubleshooting	BOR	BOR
Shift 4 Wednesday 6-6-13	Warmup/ Conditioning	Warmup/ Conditioning	BOR	BOR	BOR	Model Change	Model Change	Troubleshooting	BM1
Shift 5 Thursday 6-7-13	Warmup/ Conditioning	BM1	BM1	BM1	BM1	Model Change	Model Change	Model Change	Model Change
Shift 6 Friday 6-8-13	Warmup/ Conditioning	PM1	PM1	PM1	PM1	PM1	Uninstall	Uninstall	

Figure 4-8. NASA ARC 11-Foot Wind Tunnel exploratory test calendar.

Test Hardware

The NASA ARC exploratory test made use of existing models and pressure rail instrumentation. The larger performance model was used for boom and force testing, while the smaller boom model was used for boom testing at larger rail separation distances. The AS2 body of revolution model was also tested as a reference. The 14-inch pressure rail was used for all testing. The support hardware consisted of the large model roll mechanism (LMRM), linear actuator, and the SR-205 sting. The LMRM was mounted to

the facility pitch/traverse strut. The rail was installed in the floor, however the position was constrained due to floor substructure. The resulting rail and model position was adequate for the exploratory test purposes and also allowed Schlieren imaging.

Figure 4-9. PM Model Installed in the NASA ARC 11-Foot Wind Tunnel.

Test Results

At the beginning of the test during the envelope expansion study, it became apparent that there were significant support-system-induced dynamics that would limit the maximum Mach number for testing. The support system dynamics caused balance limits to be reached due to the inertial loads of the model. Thus, the heavier the model, the sooner the balance limits would be reached as Mach is increased. The maximum Mach numbers achieved for the different models were:

- AS2 body of revolution ≤ 1.31
- Boom Model BM1 ≤ 1.25
- Performance Model PM1 ≤ 1.2

These maximum attainable Mach numbers for the boom and performance models are at the lower end of the Mach range of interest. However, the amount of model motion observed due to support system dynamics made the accuracy of any data collected suspect (pressure or force).

Figures 4-10 and 4-11 show results for the AS2 and BM1 models at their respective maximum achievable Mach numbers. Both z-sweeps and x-sweeps were done for spatial averaging, and both are shown on the plots. The difference in the averaged results of the x- and z-sweeps looks minimal for AS2. However, it appears that the z-sweep gives better results for the boom model.

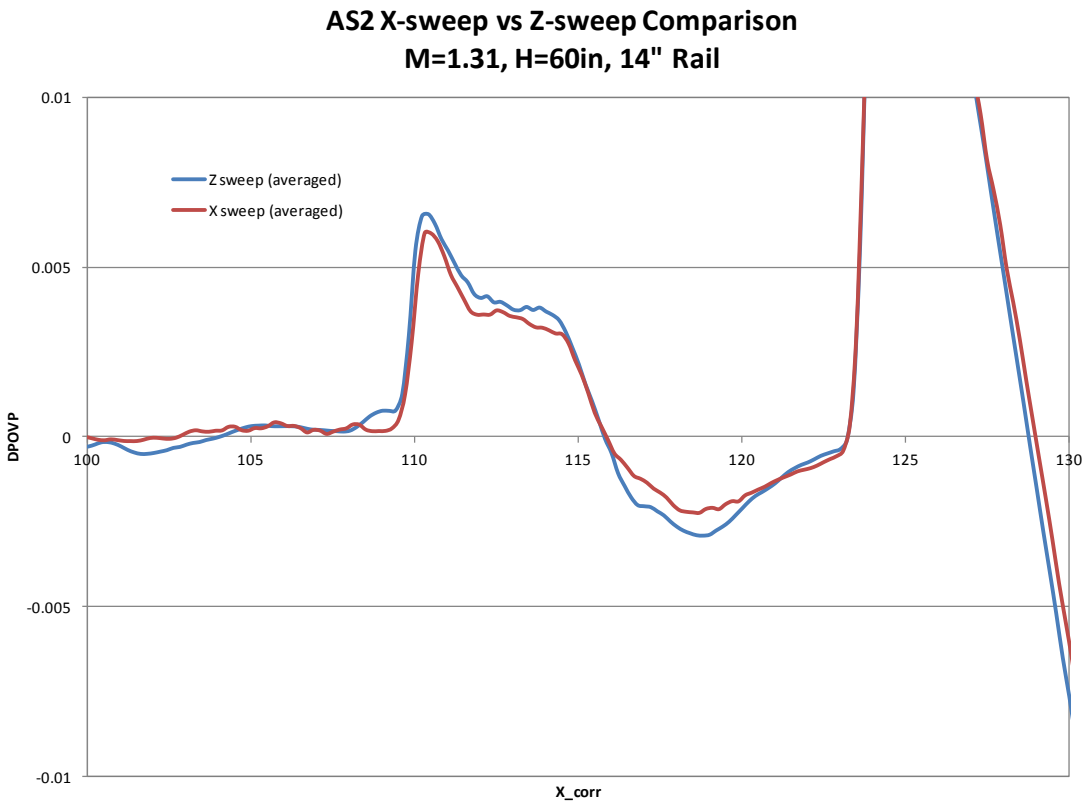

Figure 4-10. NASA ARC 11-Foot exploratory test results for AS2.

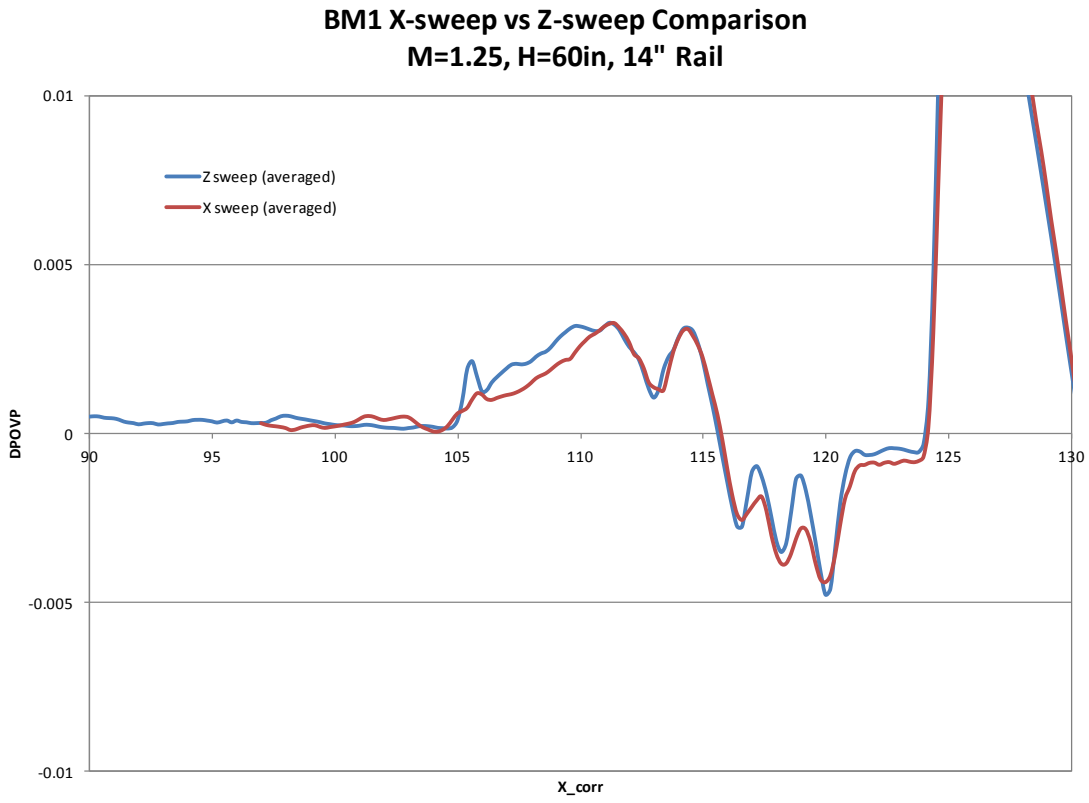

Figure 4-11. NASA ARC 11-Foot exploratory test results for the BM model.

Productivity of the NASA ARC 11-Foot Wind Tunnel was slightly difficult to gage due to support system dynamics issues. However, for test conditions without dynamics, the data acquisition rate was on par with previous 9 x 7-Foot Wind Tunnel testing metrics.

Lessons Learned

The end result of the ARC 11-Foot exploratory test was that the facility, in its current condition with the support system setup utilized, could not be used for boom or force testing as was intended. Further troubleshooting to identify the root cause of the issue was beyond the scope of the exploratory test and was not pursued. For those conditions where dynamics were not an issue, the wind-tunnel productivity seemed to be about the same as the NASA ARC 9 x 7-Foot Wind Tunnel. Although the data gathered from the 11-Foot was suspect, the test did serve the purpose of identifying any potential facility issues. The Ames facilities personnel are working on identifying the issues and are moving towards a plan to resolve them.

5 PROPULSION VALIDATION TESTING

5.1 Test Objectives

The propulsion validation testing had the following test objectives:

- Gather inlet performance data installed on the PM1 model with and without bleed
- Gather inlet performance data isolated with and without bleed
- Use the test data to calibrate CFD tool estimates

The NASA GRC 8 x 6-Foot propulsion validation test covered only the propulsion rig testing portion of the Phase II testing program. Force and boom testing were done in a separate test entry at the NASA ARC 9 x 7-Foot Wind Tunnel.

5.2 Test Calendar

The NASA GRC 8 x 6-Foot propulsion testing was scheduled as early as possible in the year in order to take advantage of the cooler temperatures to mitigate any of the dry air issues that were encountered during the exploratory test. During the test window of March 19–28, 2013, the temperatures were favorable and were typically lower than average, which resulted in almost no productivity issues due to a shortage of dry air.

	Shift Hour							
	1	2	3	4	5	6	7	8
Shift 1 Tuesday 3-19-13	Installation	Envelope Clearance	Envelope Clearance	Non-Bleed Inlet	Non-Bleed Inlet	Non-Bleed Inlet	Non-Bleed Inlet	Non-Bleed Inlet
Shift 2 Wednesday 3-20-13	Bleed Study	Bleed Study	Bleed Study	Bleed Study	Bleed Study	Bleed Study	Bleed Study	Bleed Study
Shift 3 Thursday 3-21-13	Bleed Study	Bleed Study	Bleed Study	Bleed Study	Bleed Study	Bleed Study	Bleed Study	Bleed Study
Shift 4 Friday 3-22-13	Bleed Inlet Data Matrix	Bleed Inlet Data Matrix	Bleed Inlet Data Matrix	Bleed Inlet Data Matrix	Bleed Inlet Data Matrix	Bleed Inlet Data Matrix	Bleed Inlet Data Matrix	Bleed Inlet Data Matrix
Shift 5 Monday 3-25-13	Bleed Inlet Data Matrix	Bleed Inlet Data Matrix	Bleed Inlet Data Matrix	Bleed Inlet Data Matrix	Bleed Inlet Data Matrix	Bleed Inlet Data Matrix	Bleed Inlet Data Matrix	Bleed Inlet Data Matrix
Shift 6 Tuesday 3-26-13	Bleed Inlet Data Matrix	Bleed Inlet Data Matrix	Bleed Inlet Data Matrix	Bleed Inlet Data Matrix	Bleed Inlet Data Matrix	Bleed Inlet Data Matrix	Bleed Inlet Data Matrix	Bleed Inlet Data Matrix
Shift 7 Wednesday 3-27-13	Isolated Inlet	Isolated Inlet	Isolated Inlet	Isolated Inlet	Isolated Inlet	Isolated Inlet	Isolated Inlet	Isolated Inlet

Figure 5-1. Propulsion validation test calendar.

5.3 Test Specific Hardware

The propulsion rig hardware built for the N+2 validation test consisted of an inlet attached to an instrumented AIP section connected to a mass flow plug. The rig was designed such that it attached to the existing performance model to form an installed nacelle configuration and could be configured without the model for an isolated installation. The scale of the propulsion rig (and inlet) was about 20 percent larger than the performance model. This is because the mass flow plug and AIP section were sized to the same dimensions as a previously tested set of hardware that produced acceptable results (ref. 3). The propulsion rig hardware fitted only on one side of the model (right-hand side). During propulsion rig testing, the model balance was locked out and sleeves were fitted around the sting to provide the attachment points for the propulsion rig assembly. Figure 5-2 shows the propulsion rig parts and how they were installed on the performance model.

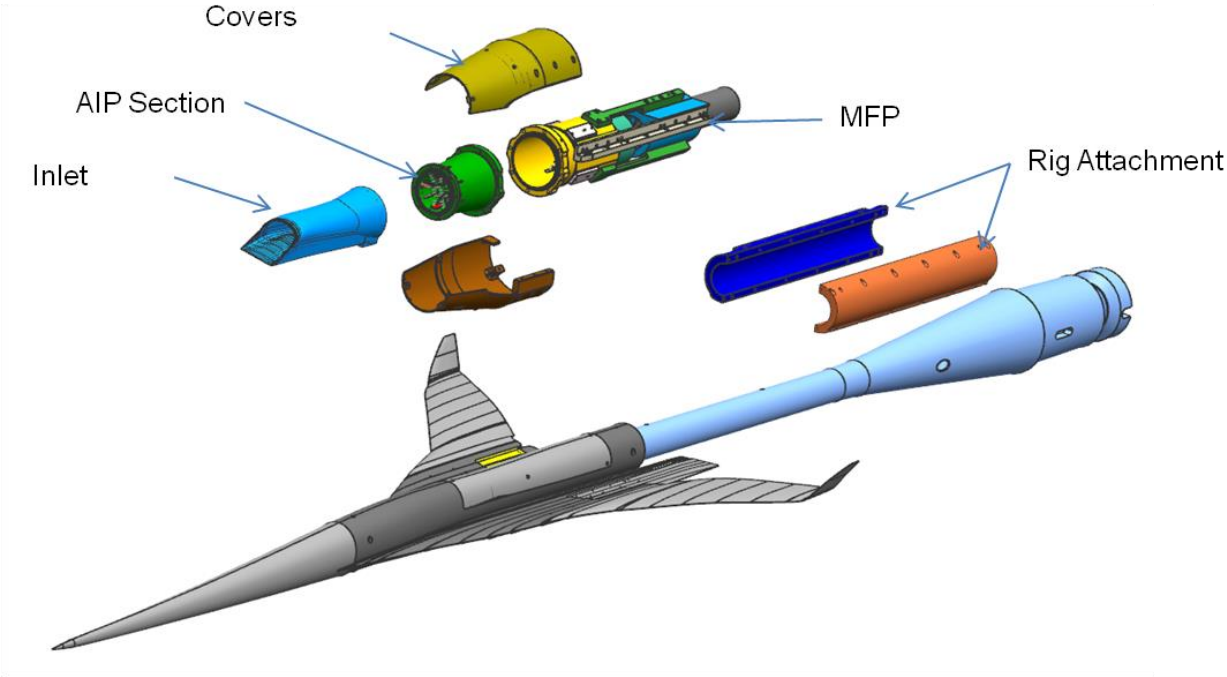

Figure 5-2. Propulsion rig parts for the PM model.

The mass flow plug was electrically actuated and used an LVDT for position sensing. The body of the mass flow plug contained four pressure rakes with three total pressures and one thermocouple per rake. Four rows of three static ports were also installed in the walls, spaced 90° apart.

The NASA GRC 8 x 6-Foot Wind Tunnel strut allows only vertical translation and angle-of-attack variation, so in order to get the required angle of attack and yaw combinations, the Ames Small Model Roll Mechanism (SMRM) was utilized. The SMRM was attached to the 8 x 6-Foot strut with an adaptor block. The sting also had strain gauges installed and wind-off check loads were performed to estimate the model deflection under load.

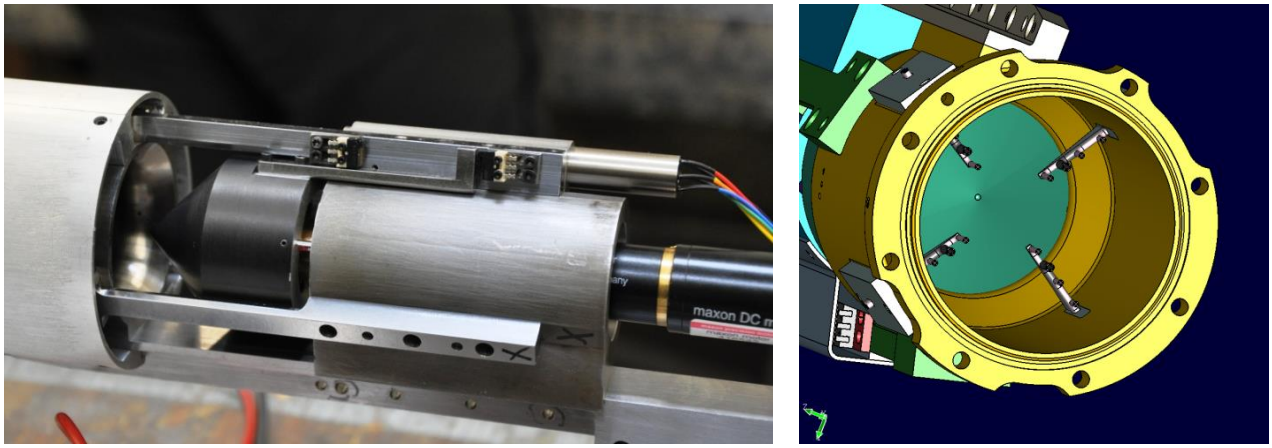

Figure 5-3. Mass flow plug body and plug.

The AIP section of the propulsion rig contained 40 total pressures arranged in eight rakes with five ports per rake. The total pressure tubes had an outer diameter of 0.032 inches, and an inner diameter of 0.014 inches. The probes were arranged radially to be at the centroids of equal areas per SAE ARP1420. Additionally, 4 kulites were installed and arranged 90° apart, and eight static pressure ports were placed at the wall in-between the pressure probe rakes. Covers were installed over the tubing for protection.

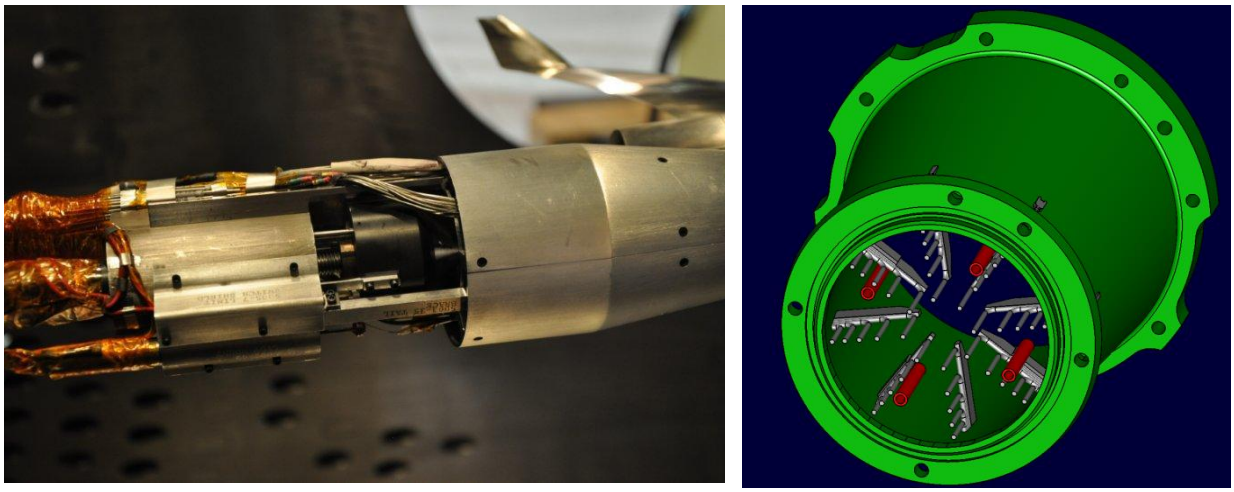

Figure 5-4. AIP covers and instrumentation.

Two inlets were made for the propulsion rig, one with a solid duct (non-bleed), and one with four bleed areas – left sidewall, right sidewall, inlet ramp, and inlet diffuser. Both inlets were built from the same loft definition. Inlet bleed areas were made by drilling a pattern of 0.02 inch through-holes. The inlet and ramp bleed sections each had a plenum chamber with exhausts ports on either side of the inlet. The bleed inlet contained seven static ports – on each sidewall along the duct and external surface, one in each of the plenum chambers, and one in the inlet duct between the ramp and diffuser bleed sections. Controlling which bleed areas were "active" was done by taping or using plaster to block the bleed holes. Figure 5-5 shows the bleed inlet and propulsion rig installed on the PM model.

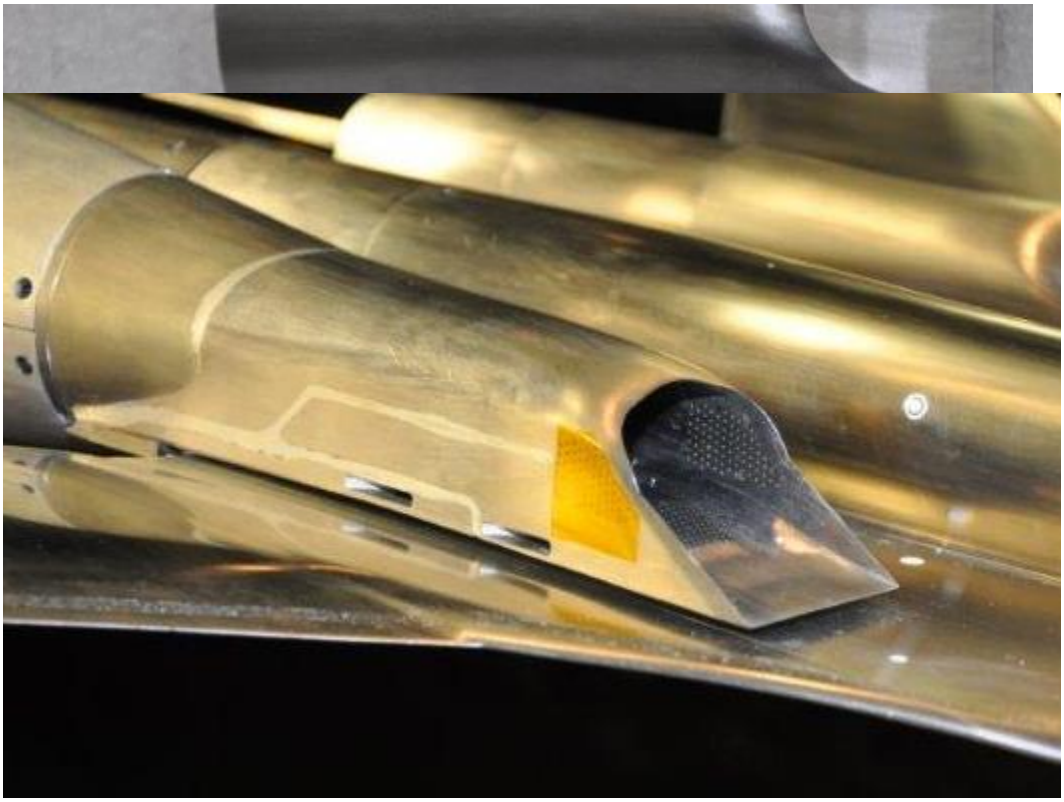

Figure 5-5. Bleed inlet and propulsion rig installed on the PM model.

5.4 Test Results

As shown in the Test Calendar (Figure 5–1), the propulsion rig test covered about 7 shifts and was split into three distinct portions – non-bleed inlet, bleed inlet, and isolated inlet testing. The non-bleed inlet portion provided a basis of comparison for the bleed inlet to ensure that the basic inlet duct performance was the same. The bleed inlet testing comprised of a study to determine the bleed characteristics of the inlet, and the best bleed configuration was then used for an expanded set of conditions. At each condition (i.e., fixed Mach, alpha, and beta), a plug sweep of 20 – 25 discrete plug positions was done to characterize the inlet performance.

Prior to the NASA GRC 8 x 6-Foot Wind-Tunnel entry, the mass flow plug was calibrated at the Boeing Flight Simulation Chamber (FSC) facility. After the calibration was complete, it was discovered that some tubing in the facility total pressure rake arrays had disconnected during the calibration, resulting in a

potential mass flow loss. Based on CFD results the effect of the disconnected tubing was estimated to be small. A post-test recalibration was done at the Boeing FSC facility to verify the results. Figure 5-6 shows the results from the MFP re-calibration at the FSC. The re-calibrated data was used in the charts presented in this report.

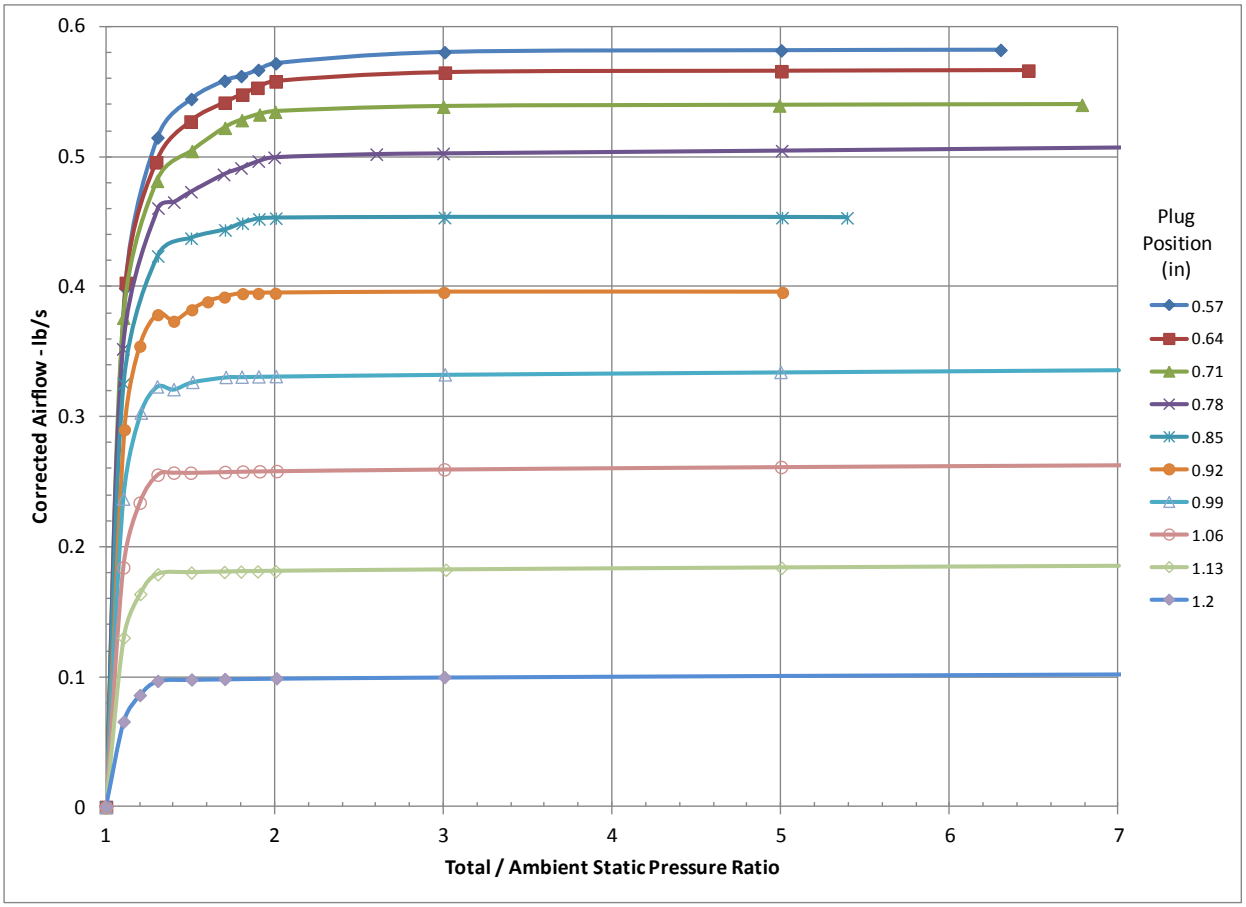

Figure 5-6. Mass flow plug calibration results.

During the bleed study, different combinations of the bleed areas were tested in order to get an idea of the most efficient bleed configuration. Figure 5-7 shows the results of the bleed study plotted as a trade between the benefit of a higher pressure recovery versus the penalty of the bleed drag. The break-even curve assumes 50 percent of the bleed momentum recovery and typical gas turbine engine sensitivity to pressure recovery at Mach 1.6. The highest pressure recovery was achieved with the ramp and diffuser bleed configuration, but the diffuser-only bleed is better overall because it is the further away from the break-even curve. Based on these results, the diffuser-only bleed configuration was used to gather a database of Machs, alphas, and beta conditions.

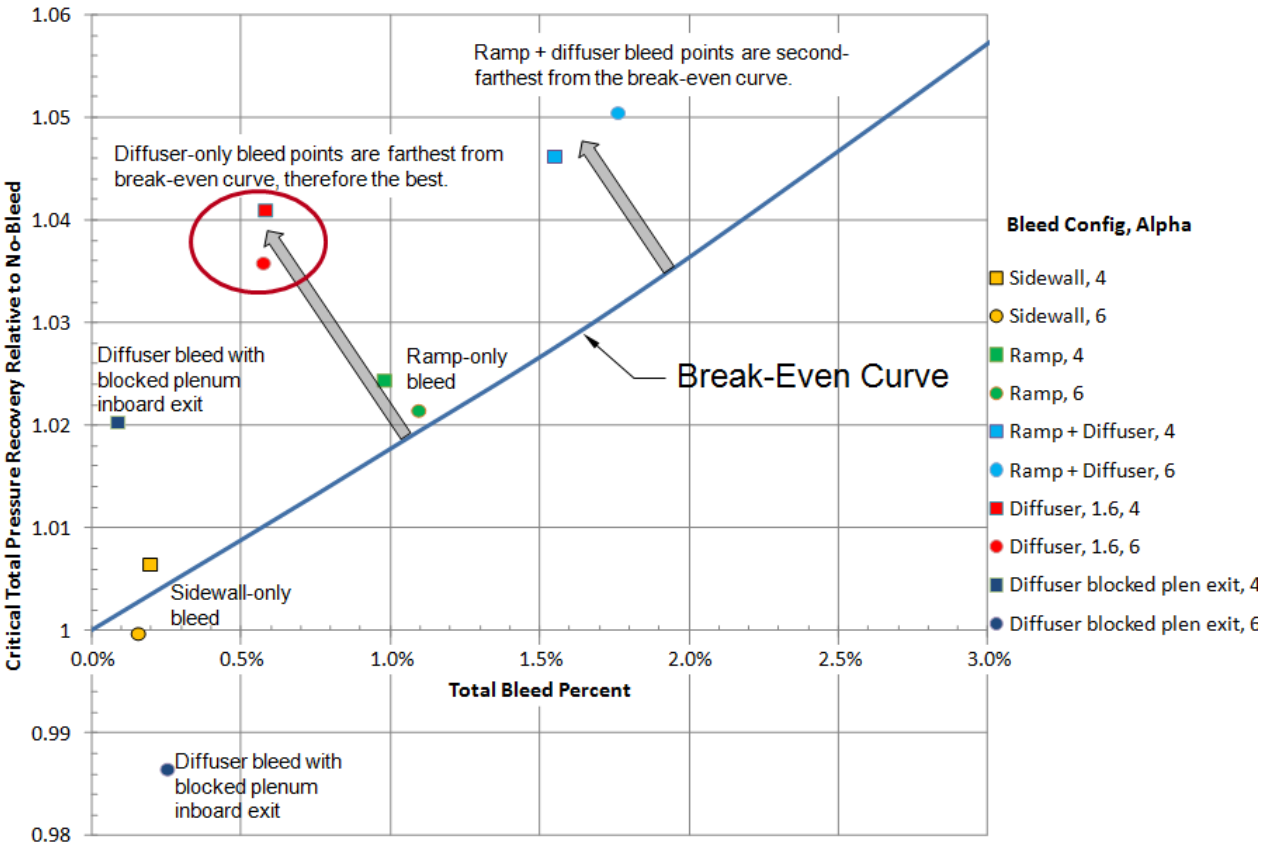

Figure 5-7. Bleed study results.

Figure 5-8 shows the critical total pressure recovery for the diffuser-only bleed configuration. The chart shows the effect of the bleed, the installation effect (vs. isolated), as well as comparisons against the Mil-Spec and published data for an F-8 Crusader inlet. This chart shows that for a relatively small amount of bleed (<1 percent), the inlet recovery is improved by about 3 percent. For most of the Mach range, the

inlet with bleed has a recovery similar to the F-8 (a past supersonic aircraft) inlet. For Mach numbers less than 1.2, the installation effect is minimal, and for Mach numbers greater than 1.4, the isolated inlet has a recovery similar to the Mil-Spec curve.

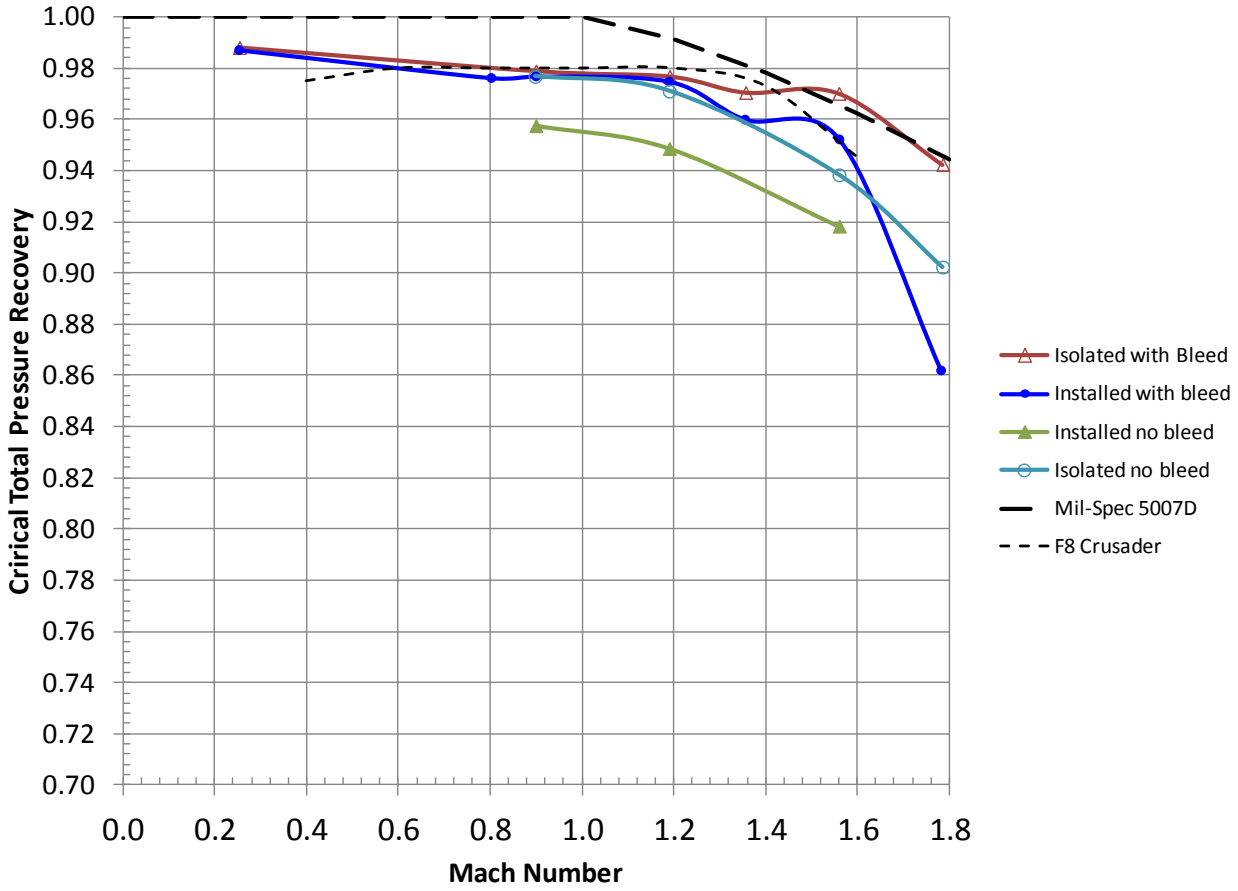

Figure 5-8. Critical total pressure recovery.

Figure 5-9 shows the variation of the critical total pressure recovery with alpha and beta. From this chart, it can be seen that there is very little decrease of the pressure recovery with increasing angle of attack up to 4°, but it starts to degrade significantly at higher angles of attack. Also, the adverse sensitivity of pressure recovery to sideslip angle starts increasing above 4° angle-of-attack (note – the QEVC supersonic cruise angle-of-attack is less than 4°).

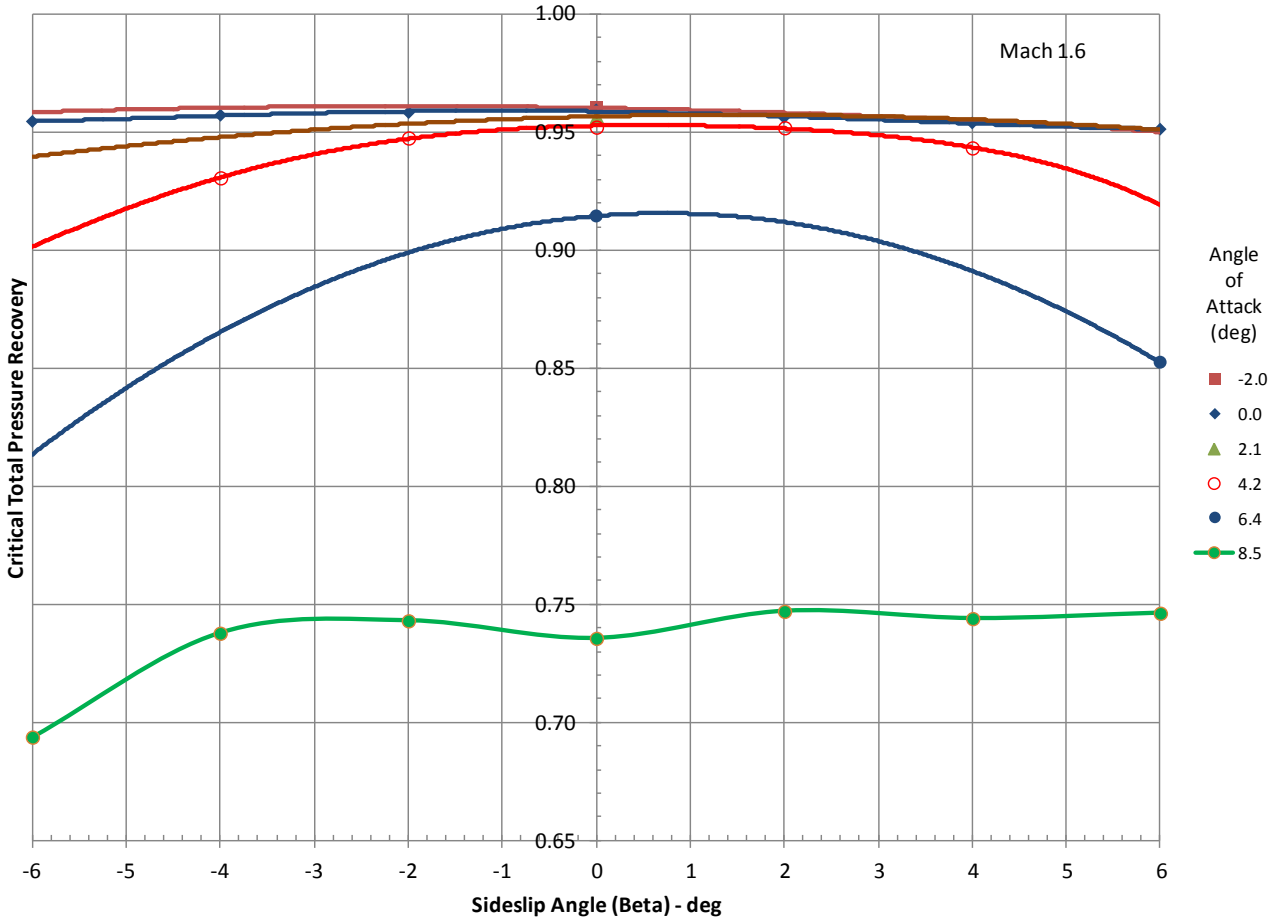

Figure 5-9. Effect of angle of attack and sideslip on critical total pressure recovery.

Figure 5-10 shows the variation of distortion (KD2) with alpha and beta at the point of critical inlet operation. This chart shows that there is little increase in distortion with increasing angle of attack up to 4° , but it starts to degrade significantly at higher angles of attack. The adverse sensitivity of distortion to sideslip angle starts increasing above 4° angle of attack.

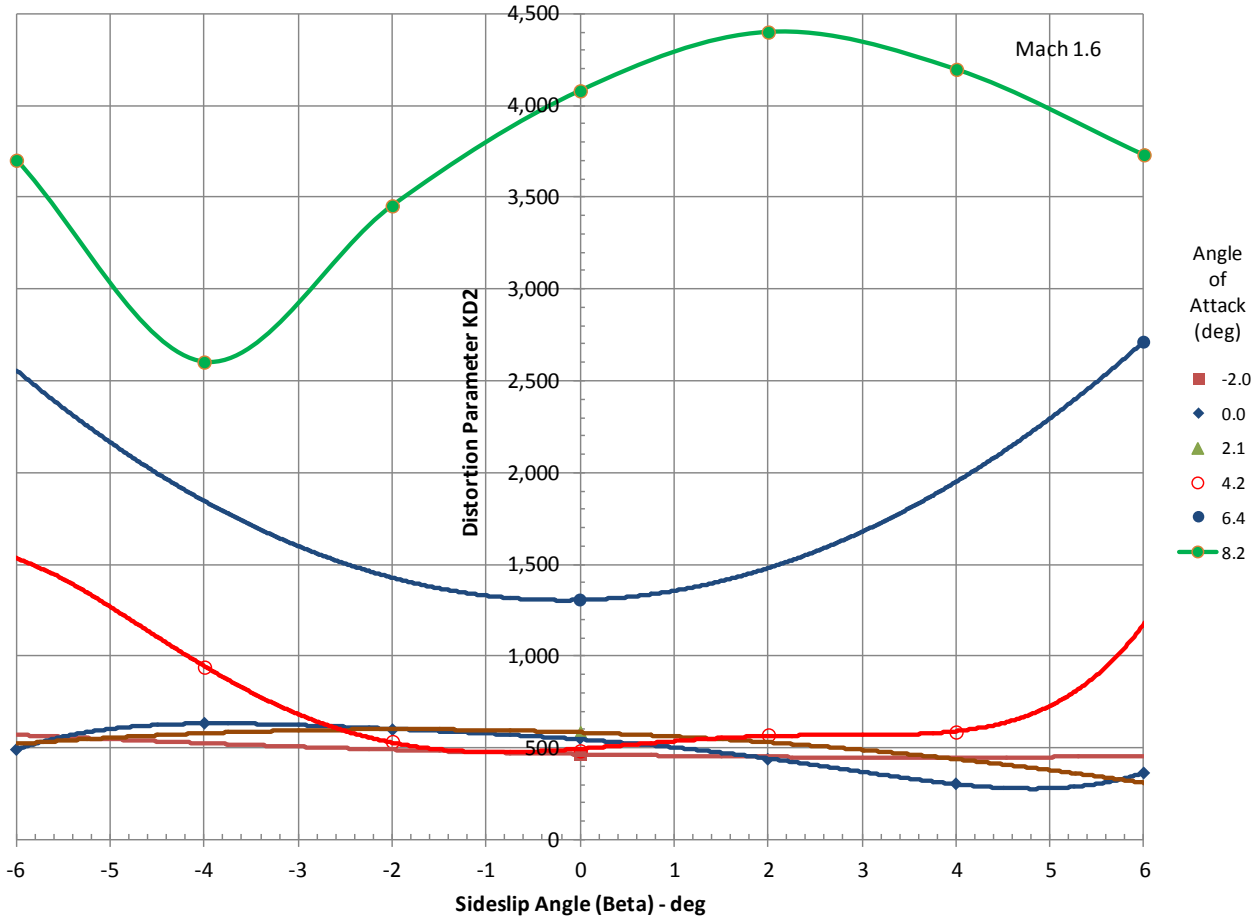

Figure 5-10. Effect of angle of attack and sideslip on distortion (KD2).

5.5 Conclusions

Results from the NASA GRC 8 x 6-Foot Wind Tunnel test showed that the over-wing inlet location with diffuser-only bleed is a viable configuration for a supersonic transport, with good operating characteristics for angles of attack less than 4°, and yaw angles less than +/- 2°. Locating the inlet on top of the wing had no measurable critical inlet total pressure recovery penalty at Mach 1.2 and lower, and showed a penalty of about 1 percent at Mach numbers of 1.6 and 1.8 at low angles of attack at yaw angles.

6 SONIC BOOM AND FORCE VALIDATION TESTING

6.1 Test Objectives

The objectives for the sonic boom and force validation testing were to:

- Gather under-track and off-track boom signals for the performance model utilizing the new modular nacelles to simulate engine power settings

- Gather under-track and off-track boom signals with the boom model at extended distances from the pressure rail utilizing the VS3 and VS4 support struts
- Gather force and moment data using the performance model
- Estimate model aeroelastics using photogrammetry techniques
- Use the test data to calibrate CFD tools

6.2 Test Calendar

Testing at the NASA ARC 9 x 7-Foot Wind Tunnel spanned about 12 shifts, including installation and removal.

	6:30-7:30	7:30-8:30	8:30-9:30	9:30-10:30	10:30-11:30	11:30-12:30	12:30-1:30	1:30-2:30
Shift 1 Monday 4/22/13	Conditioning	Conditioning	Conditioning	Conditioning	Strut Cone	Strut Cone	Install	Install
Shift 2 Tuesday 4/23/13	Install	Install	Install	Install	Install	Install	Install	Install
Shift 3 Wednesday 4/24/13	Install	Install	Install	Install	Install	Install	Install	Install
Shift 4 Thursday 4/25/13	Install	Install	Install	Install	troubleshoot	troubleshoot	troubleshoot	troubleshoot
Shift 5 Friday 4/26/13	troubleshoot	troubleshoot	troubleshoot	troubleshoot	troubleshoot	troubleshoot	troubleshoot	Performance Model

Figure 6-1. Sonic boom and force validation test calendar, Week 1.

	6:30-7:30	7:30-8:30	8:30-9:30	9:30-10:30	10:30-11:30	11:30-12:30	12:30-1:30	1:30-2:30
Shift 6 Monday 4/29/13	Conditioning	Conditioning	Performance Model	Performance Model	Performance Model	Performance Model	Performance Model	Performance Model
Shift 7 Tuesday 4/30/13	Conditioning	Conditioning / Performance Model	Performance Model	Performance Model	Model change	Model change	Performance Model	Performance Model
Shift 8 Wednesday 5/1/13	Conditioning	Conditioning / Performance Model	Performance Model	Performance Model	Model change	Model change	Performance Model	Performance Model
Shift 9 Thursday 5/2/13	Conditioning	Conditioning / Performance Model	Performance Model	Performance Model	Model change	Performance Model	Performance Model	Model change
Shift 10 Friday 5/3/13	troubleshoot	Conditioning	Conditioning	Boom Model	Boom Model	Model change	Model change	Boom Model

	6:30-7:30	7:30-8:30	8:30-9:30	9:30-10:30	10:30-11:30	11:30-12:30	12:30-1:30	1:30-2:30
Shift 7 Monday 5/6/13	troubleshoot	troubleshoot	troubleshoot	troubleshoot	Conditioning	Boom Model	Boom Model	Boom Model
Shift 8 Tuesday 5/7/13	troubleshoot	Boom Model	Boom Model	Model change	Boom Model	Boom Model	Uninstall	Uninstall
Shift 8 Wednesday 5/8/13								

Figure 6-2. Sonic boom and force validation test calendar, Weeks 2 and 3.

6.3 Test Specific Hardware

New hardware was built with the goal of being able to discern the effects of nacelle inlet spillage and nozzle plume on the boom signal. Two nacelles were designed, N3 and N4. The N3 nacelle was a nominally sized inlet with Mach 1.6 determined to be the primary operating Mach number. N4 had a 15 percent oversized inlet, along with a similarly over-expanded nozzle. These nacelles shared a common center section, and for the performance model, the inlets and nozzles between N3 and N4 parts were

interchangeable. Figures 6-3 and 6-4 show the parts for the performance model. For the boom model, two new mounting concepts were built – a mid-body mounted upper swept strut (USS, also called VS3), and an aft sting mount (VS4, Figures 6-5 and 6-6). Both of these model mounts were designed to be able to discern the nacelle and plume effects on the boom signal. Additionally, new nacelle parts for N3 and N4 were built for the boom model.

A tailored "dummy" sting was designed with a specific shape to produce a boom signature in order to better discern nacelle and model aft body effects. For the performance model, the sting contours were achieved by clamshell parts fitted over the 28-inch Boeing sting. When the contoured parts were installed, a lockout collar prevented motion of the model relative to the balance. Thus, the balance forces were invalid when the collar and clamshell sting contour parts were used. For the boom model, the contours were built-in to the sting support.

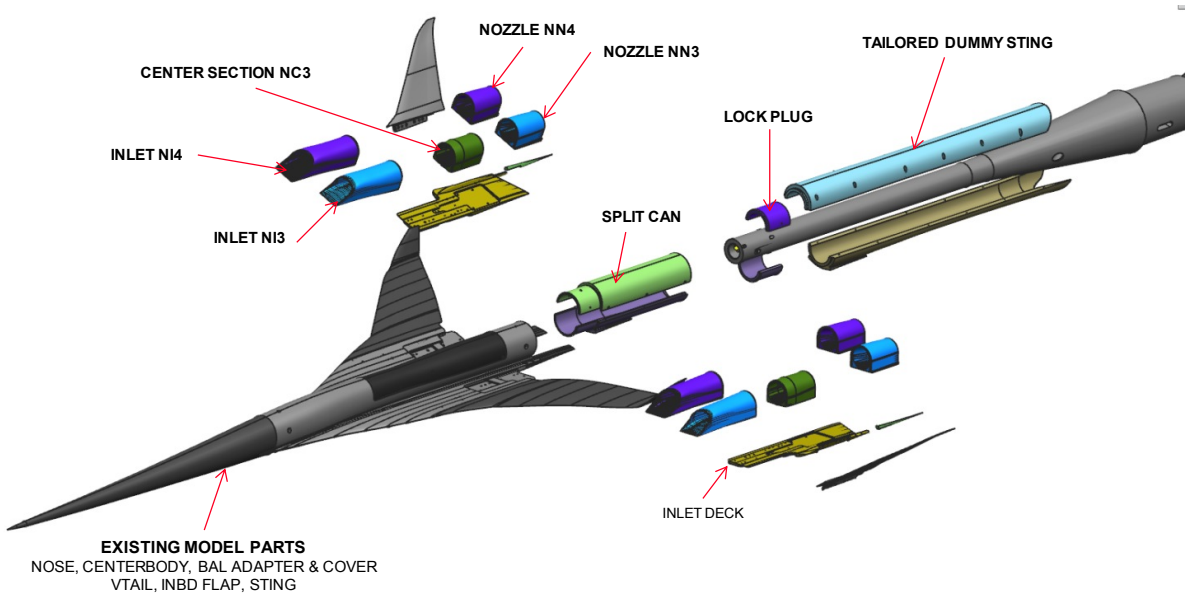

Figure 6-3. Boom and force parts assembly for the PM model.

Figure 6-4. Boom and force parts for the PM model.

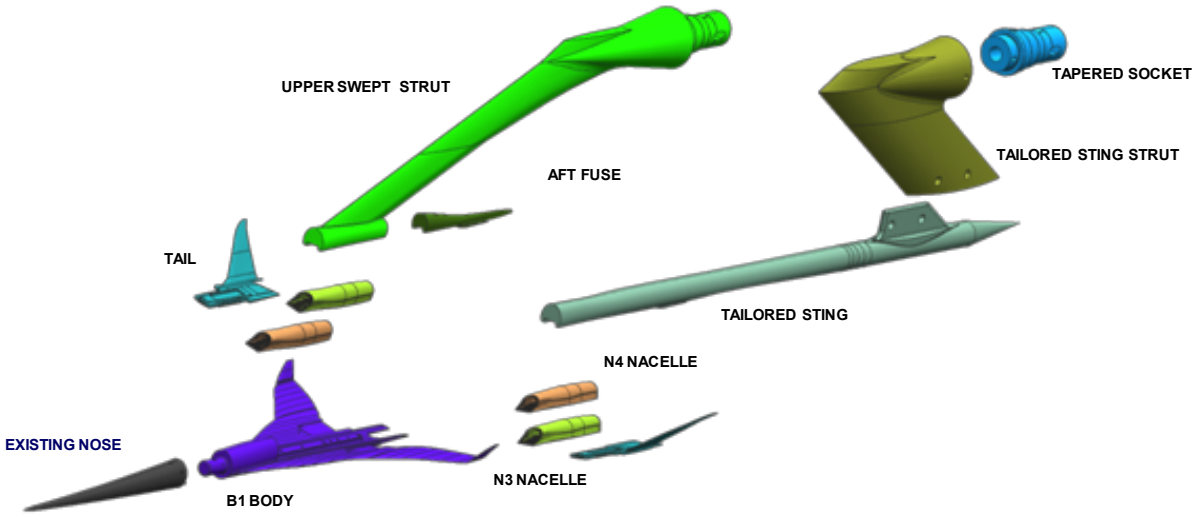

Figure 6-5. Boom parts assembly for BM model.

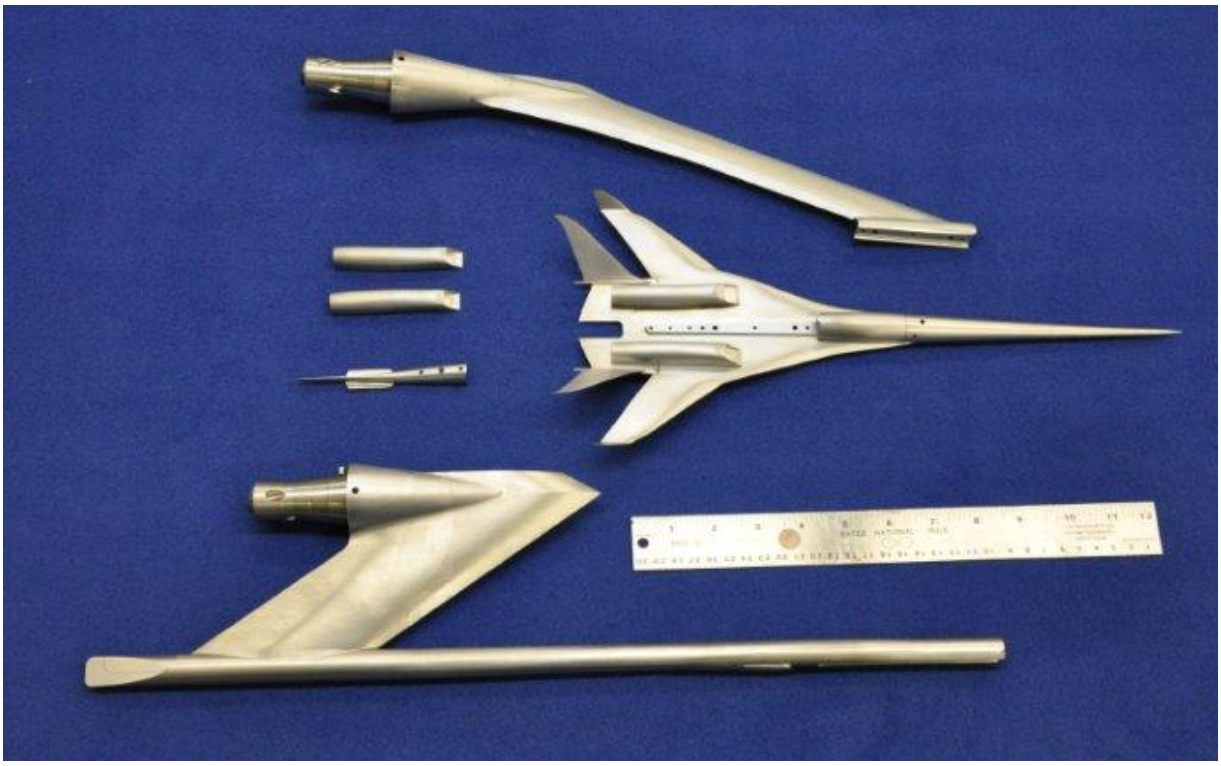

Figure 6-6. Boom parts for the BM model.

6.4 Test Results

During the past several tests at the NASA ARC 9 x 7-Foot Wind Tunnel, a basic method of boom data collection was developed. This method includes the averaging of boom signals in order to minimize the spatial and temporal variations within the tunnel, ensuring humidity levels do not exceed a specified level and keeping the humidity variation within a tolerance during running. In addition, two new methods were added – (1) bleeding dry air into the tunnel circuit when the wind- tunnel section was open or during off-shift hours in order to maintain a low humidity level and minimize conditioning time and (2) using a single clear-tunnel reference as the basis for reducing all data from the test, while striving to match the humidity of the data run to the reference run as closely as possible.

A linear actuator was not used for the model support system, so only z-sweeps were used for model movement. Model roll was achieved using the small model roll mechanism (SMRM), and off-track model positioning used the SMRM along with the facility knuckle/sleeve system. Model heights were nominally 62 inches above the rail, which resulted in h/l of about 1.4 for the performance model, and about 4.1 for the boom model.

For the boom model, initial results from the shaped sting (VS4) showed that the support system shockfront overtook the aft signature, obscuring the areas of interest. Because of this, further testing of the VS4 sting mount was dropped, and the mid-body USS (VS3) configuration was used for most of the remaining testing.

Figures 6-7 and 6-8 show results for a typical z-sweep for the performance and boom models. The traces of the individual signals indicate the need for signal averaging. The boom signals for the performance model are large enough to see some of the finer details due to the model proximity to the rail. For the

boom model at the larger h/l distances, Figure 6-8 shows that some detail has been lost due to interferences. However, this was not unexpected.

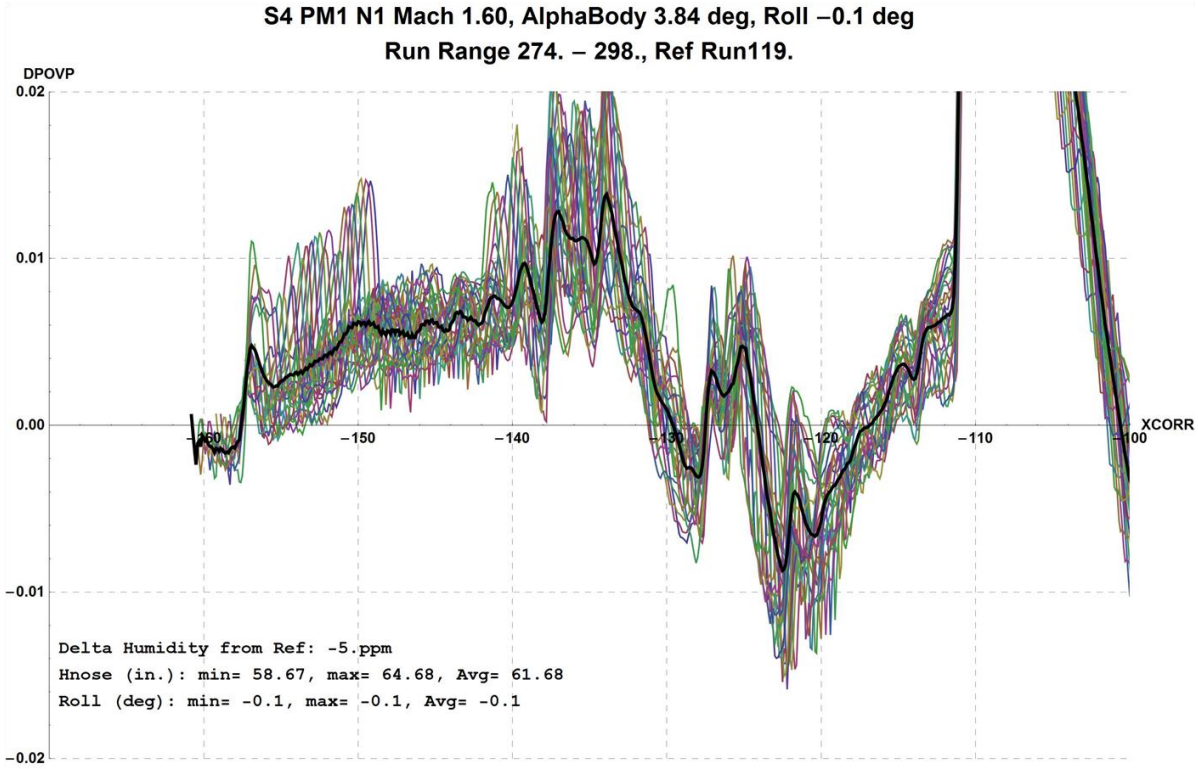

Figure 6-7. Individual and averaged boom signals, PM model.

Figures 6-9 to 6-12 show the boom signals for the PM model with nacelles N1, N2, and N3 for roll angles for 0°, 15°, 30°, and 45°. Figures 6-13 to 6-16 show the boom signals for the PM model with nacelle inlet N3 with nozzle N4, and inlet N4 with nozzle N3. Figure 6-17 shows the force and moment results for the performance model with N1 and N3 nacelles. Figures 6-18 to 6-21 show the boom signal results for the BM model with nacelles N3 and N4 with the mid-body USS mount.

During the test a photogrammetry technique was used to help determine the aeroelastic effects on the models. The results were to be used to determine a deflected shape that could be analyzed with CFD. However, the results were not available in time to do this CFD analysis before the project ended. Instead an estimated aeroelatic shape was used for this comparison. Please see section 7.2 for further details.

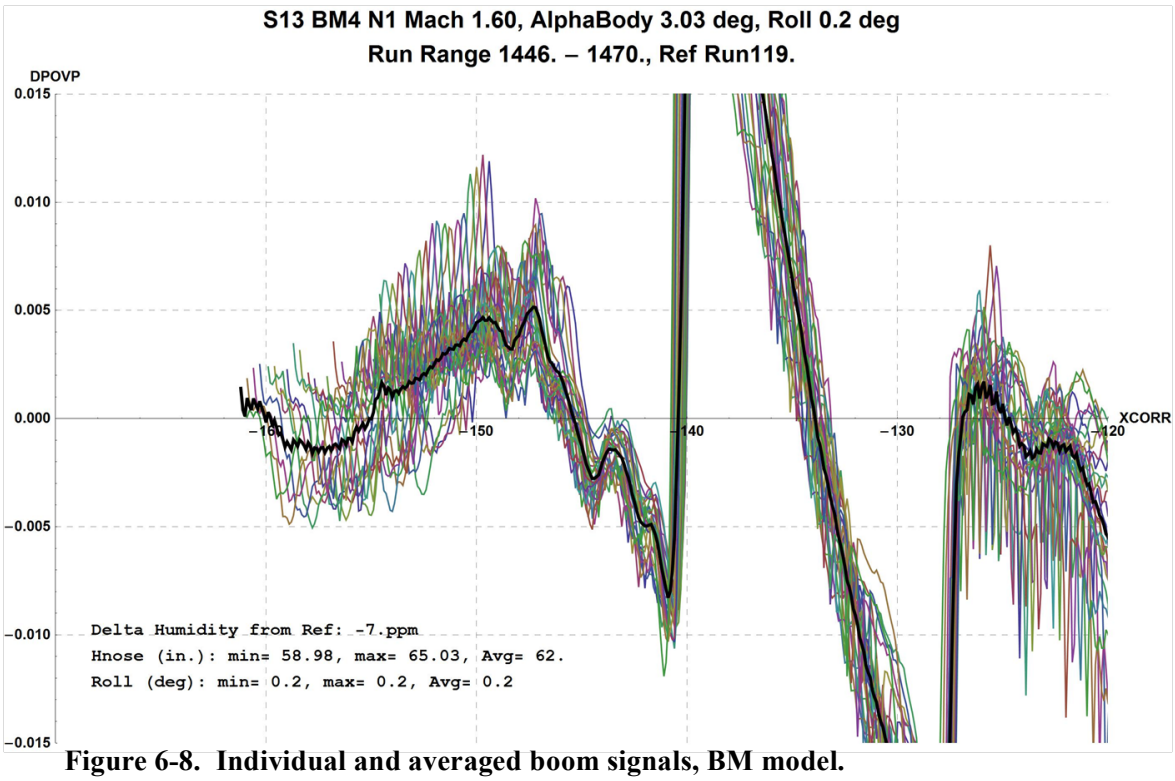

Figure 6-8. Individual and averaged boom signals, BM model.

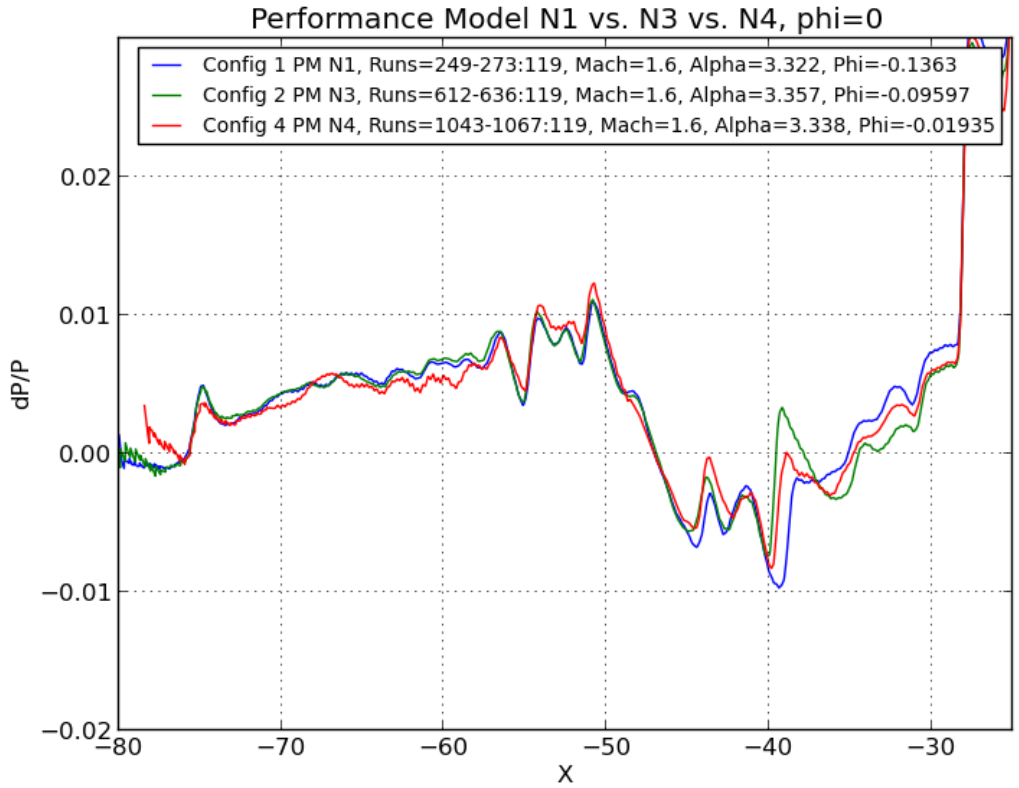

Figure 6-9. Nacelle effect on boom signal, under-track, PM model.

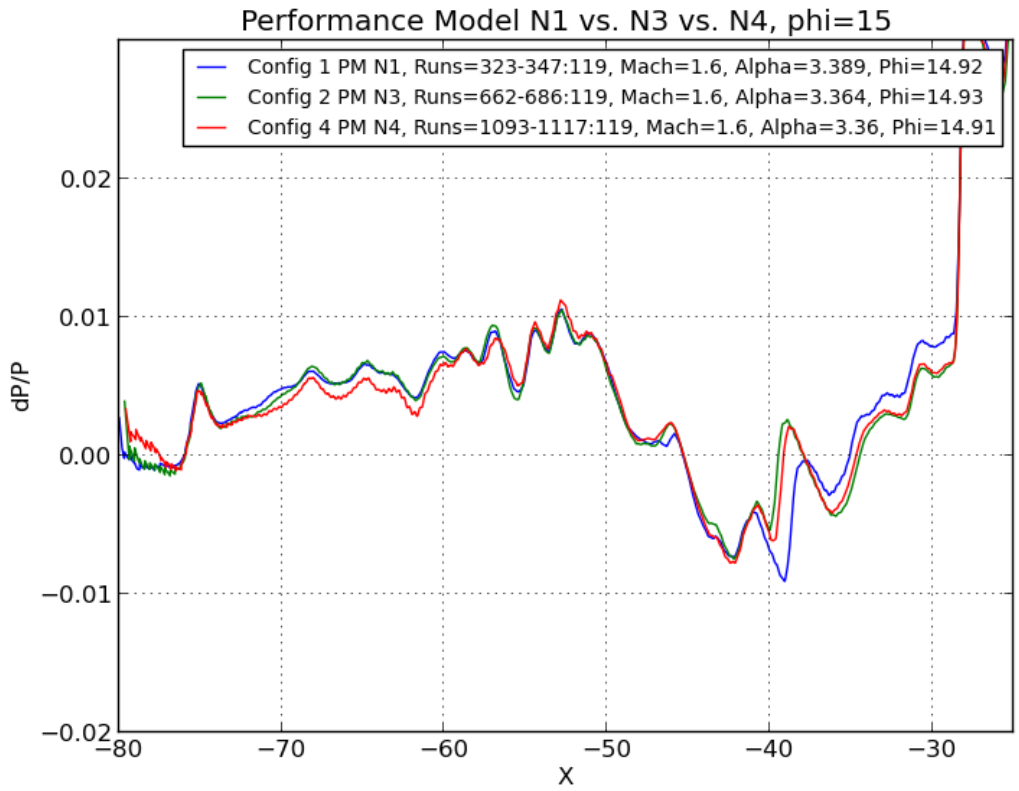

Figure 6-10. Nacelle effect on boom signal, off-track 15°, PM model.

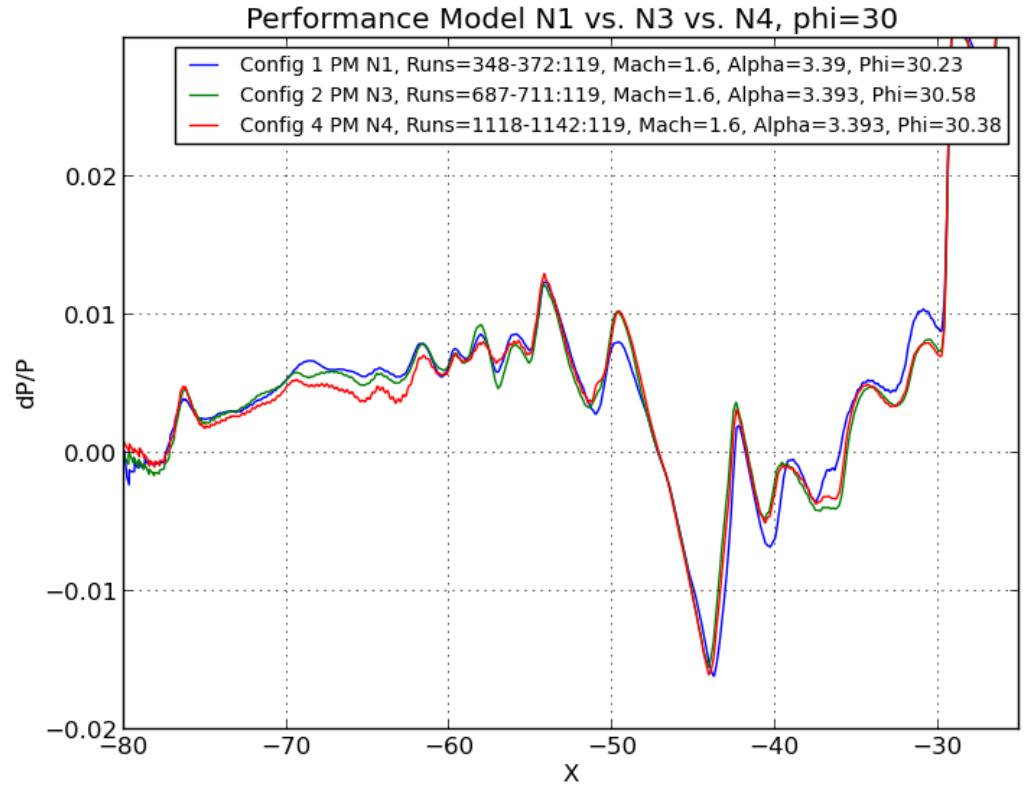

Figure 6-11. Nacelle effect on boom signal, off-track 30°, PM model.

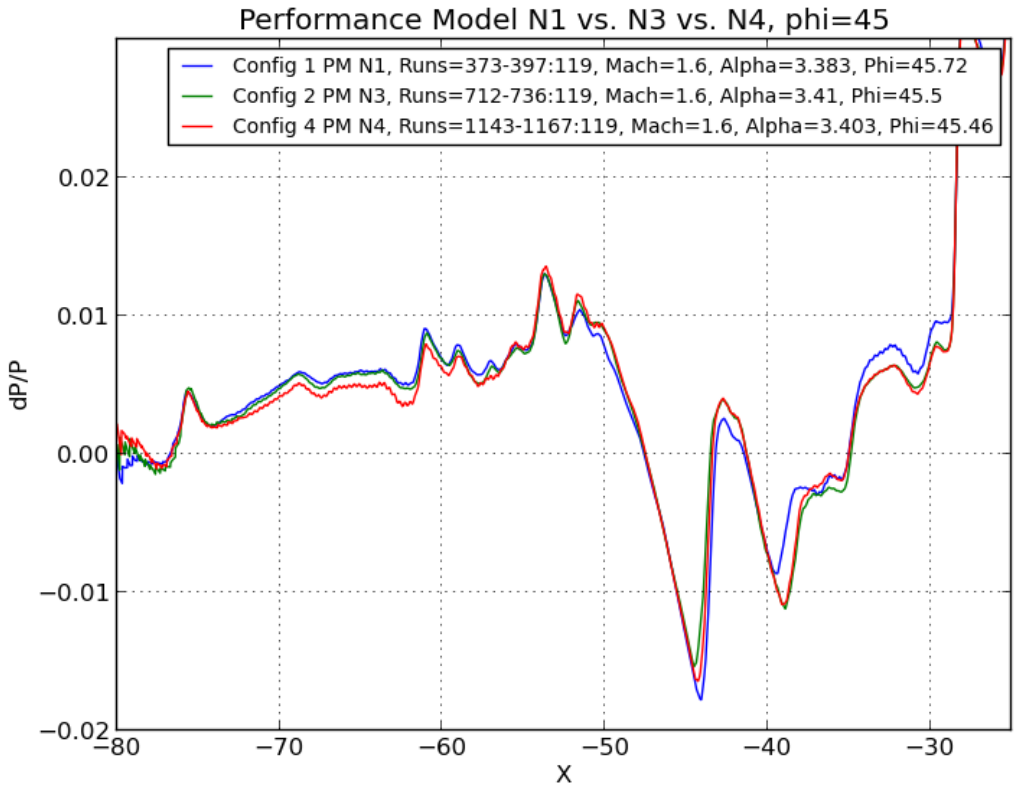

Figure 6-12. Nacelle effect on boom, off-track 45°, PM model.

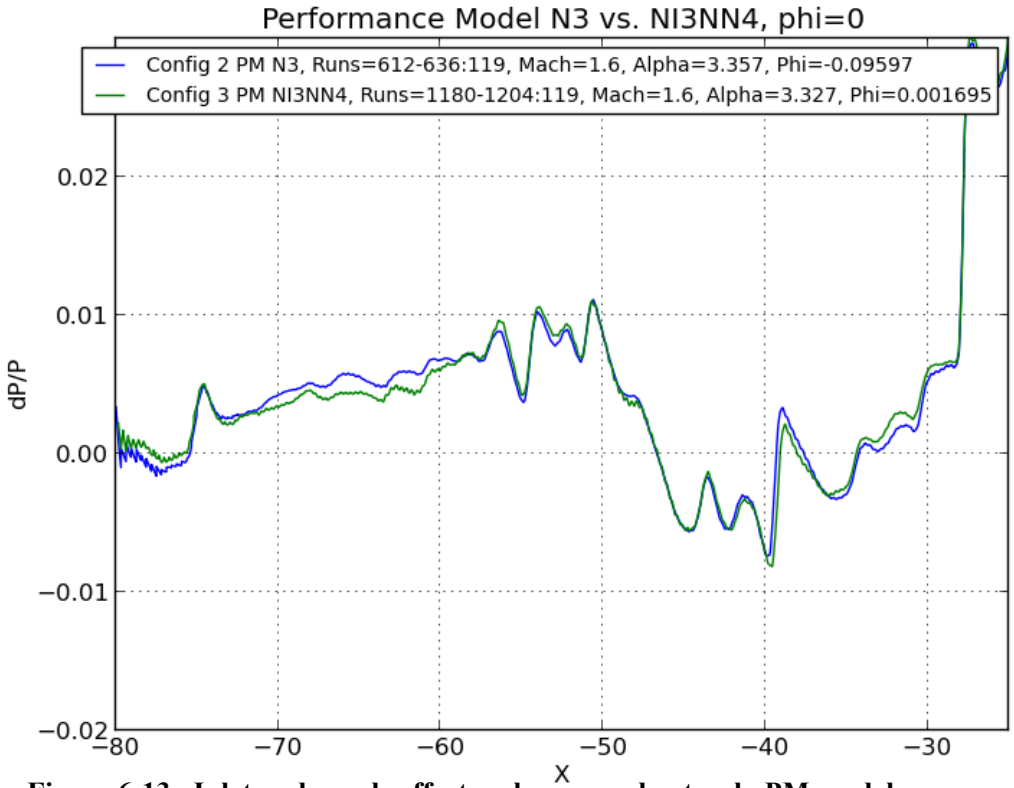

Figure 6-13. Inlet and nozzle effect on boom, under-track, PM model.

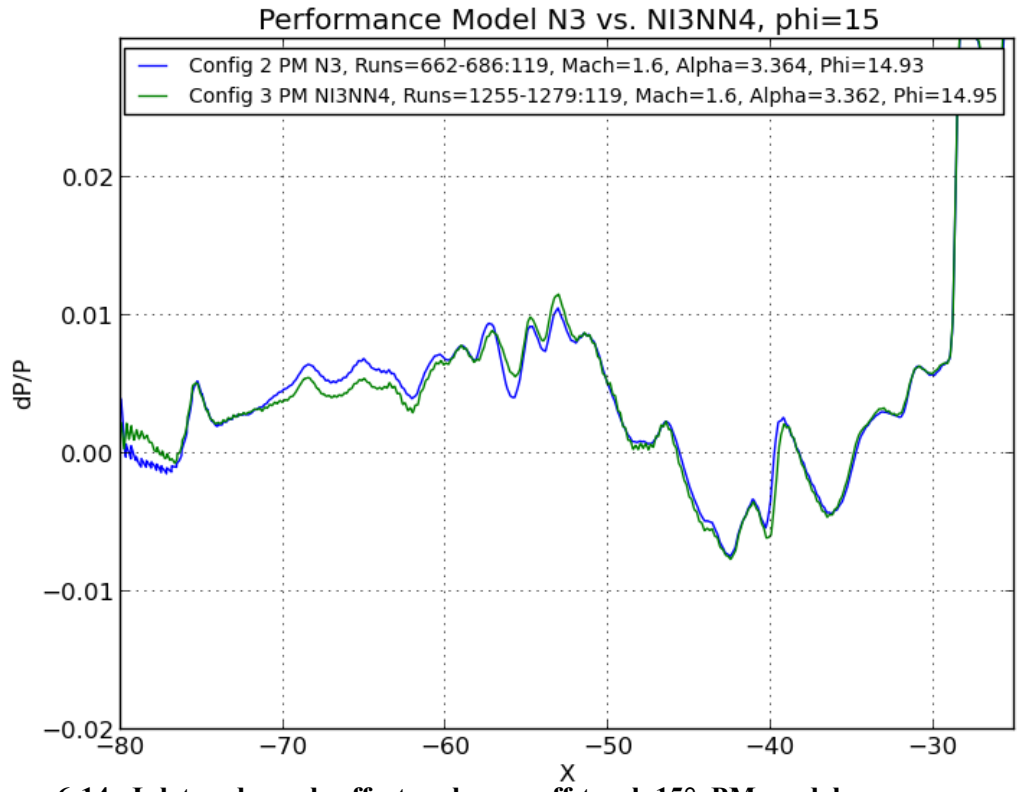

Figure 6-14. Inlet and nozzle effect on boom, off-track 15°, PM model.

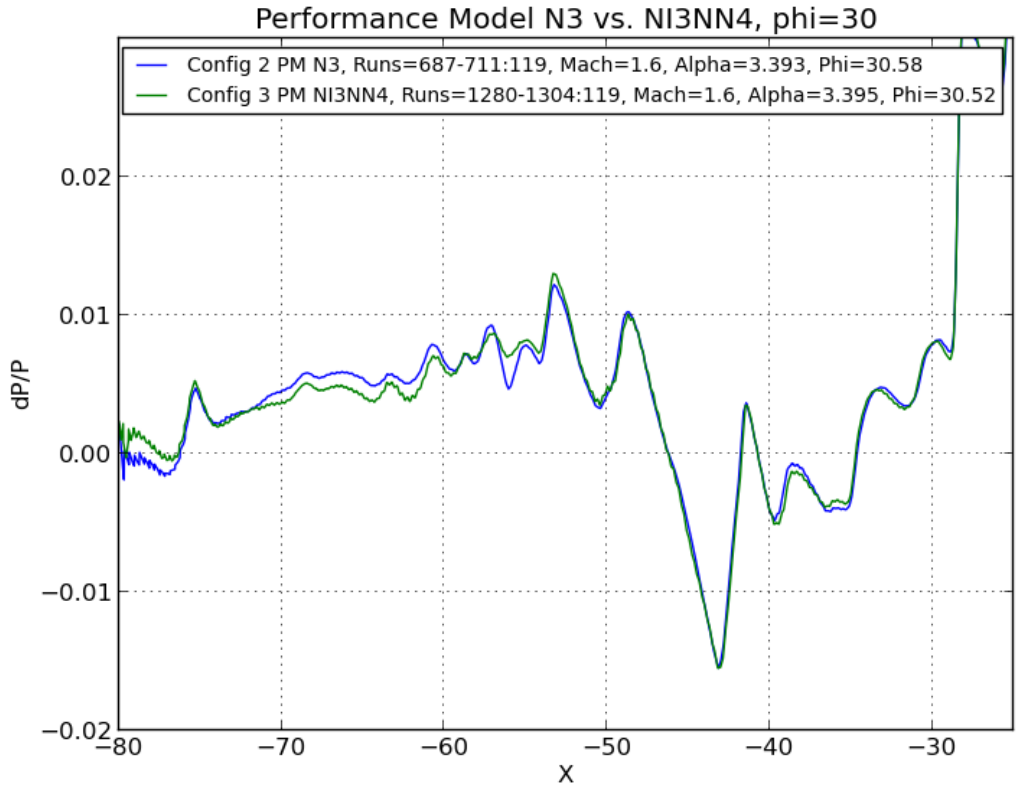

Figure 6-15. Inlet and nozzle effect on boom, off-track 30°, PM model.

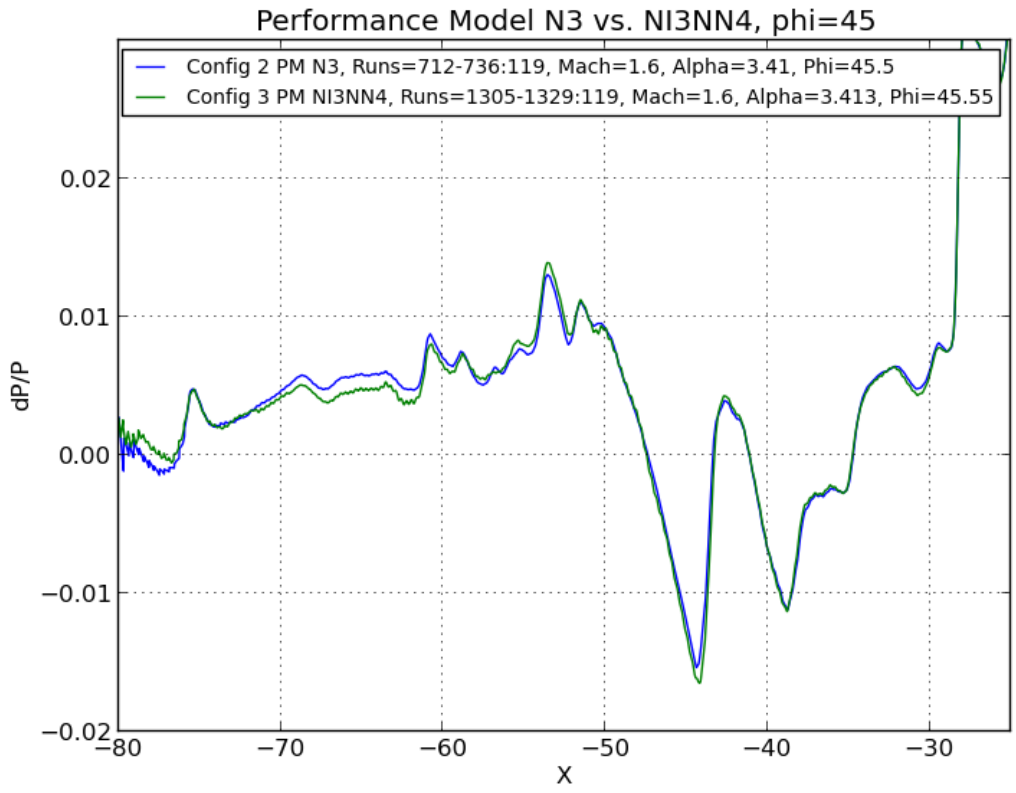

Figure 6-16. Inlet and nozzle effect on boom, off-track 45°, PM model.

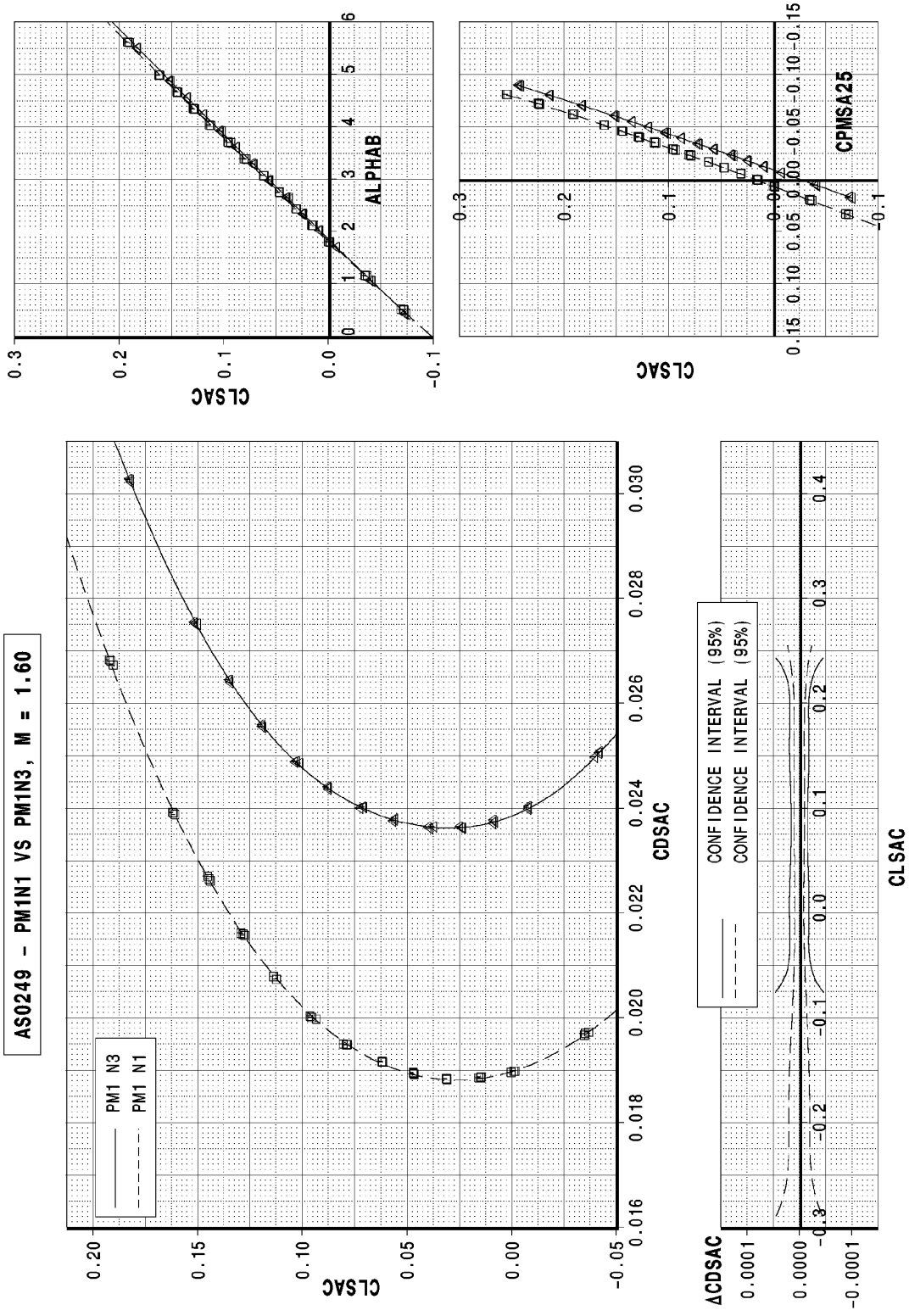

Figure 6-17. Force polars, N1 vs. N3, PM model.

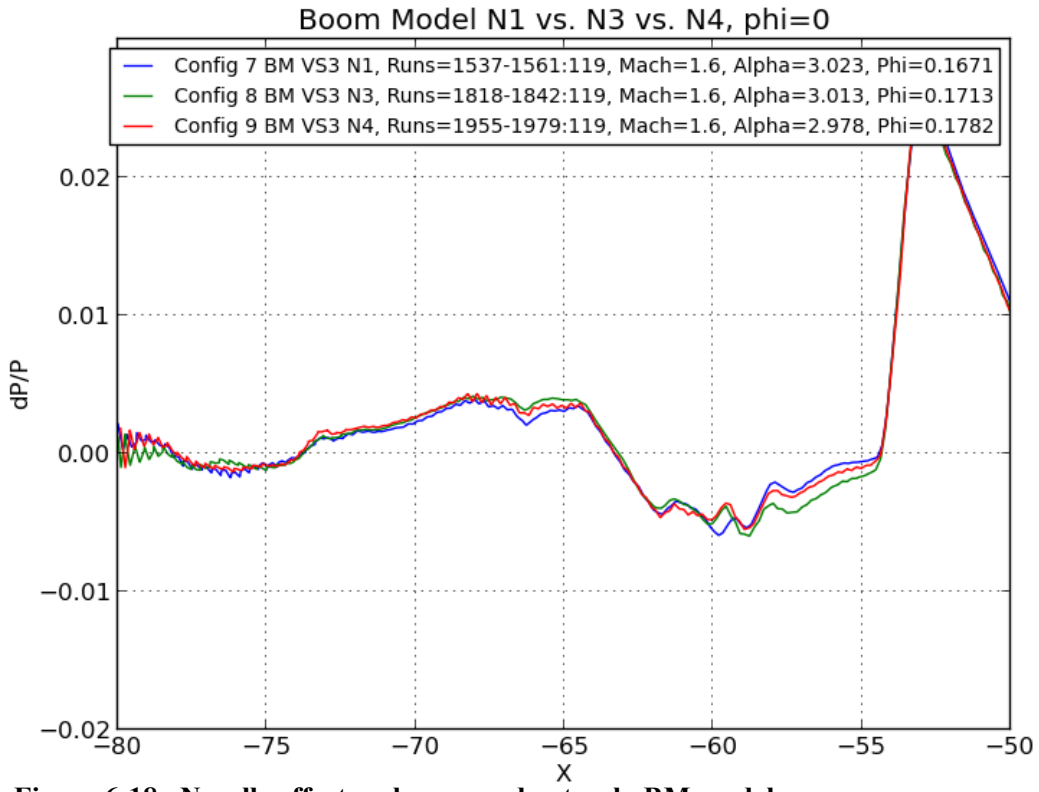

Figure 6-18. Nacelle effect on boom, under-track, BM model.

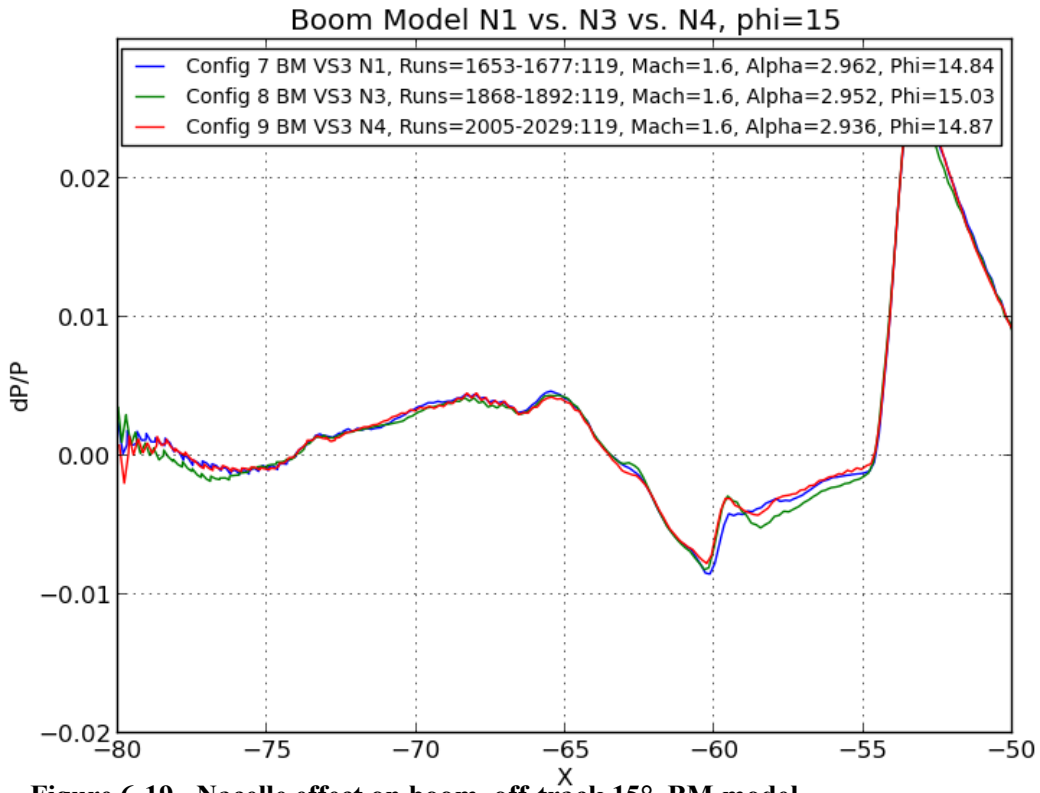

Figure 6-19. Nacelle effect on boom, off-track 15°, BM model.

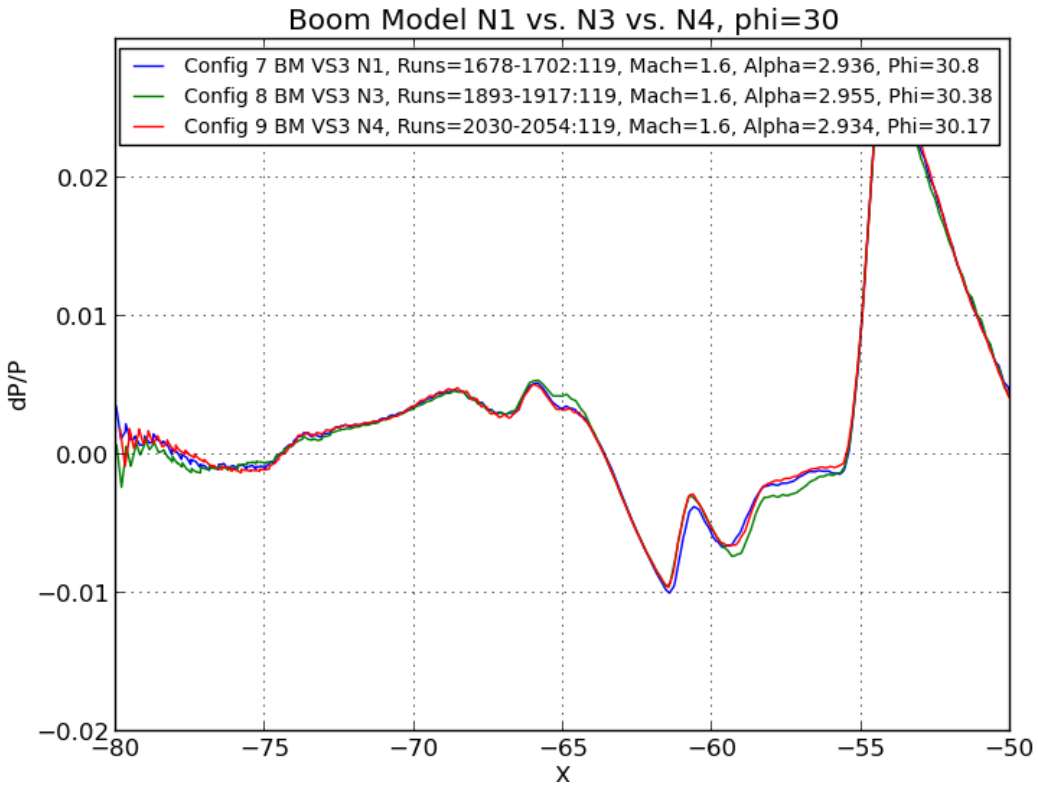

Figure 6-20. Nacelle effect on boom, off-track 30°, BM model.

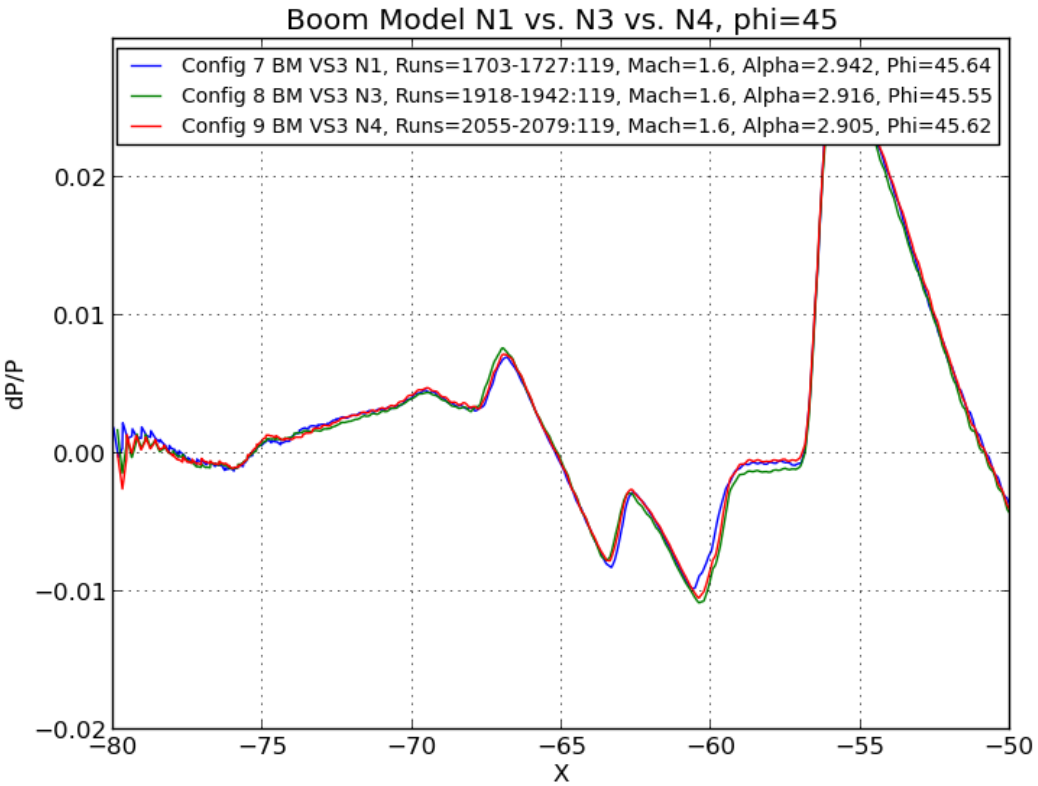

Figure 6-21. Nacelle effect on boom, off-track 45°, BM model.

6.5 Conclusions

Results from the NASA ARC 9 x 7-Foot Wind Tunnel test show that the difference between N1, N3, and N4 was minor and tend to be within data uncertainty, both under-track and off-track. Similarly, the inlet and plume effects were also minor and within data uncertainty. For the boom model, the mid-body USS mount worked as designed. However, boom model signatures at ~62 inches away show some rounding due to signal interferences.

The nominal data processing method for the test was to use a single reference run. This method seemed to provide satisfactory results as long as humidity in the data run was relatively close to that in the reference run. This should be considered in the future as a potential time-saving process. Another process that helped productivity was bleeding dry air into the tunnel section while the circuit was open. This helped minimize the amount of run time needed to get the tunnel on-condition for humidity.

7 CFD AND VALIDATION ANALYSIS

While CFD was used during the design and development of the aircraft, a further set of CFD runs was done post-test to provide a more direct comparison with experimental results. OVERFLOW was the main CFD code used for both the propulsion integration and sonic boom predictions. For a few sonic boom cases, CART3D was also used and the results were compared with OVERFLOW run in the inviscid mode.

7.1 Propulsion Integration Validation

OVERFLOW was run at wind-tunnel conditions for the propulsion rig installation as tested at the NASA GRC 8 x 6-Foot Wind Tunnel. Figures 7-1 and 7-2 show the results, comparing the total pressure ratios versus capture area ratios as well as the contour plots of the AIP at sub-critical, near-critical, and super-critical plug positions. For Mach 1.2, the OVERFLOW results generally agree with the test data and the capture ratio is about 2 percent greater. For Mach 1.6, the super-critical capture area ratio is about 4 percent greater than the test data and about 1 percent greater in total pressure ratio, while the near critical case shows good agreement between CFD and test data where the total pressure ratio is about the same.

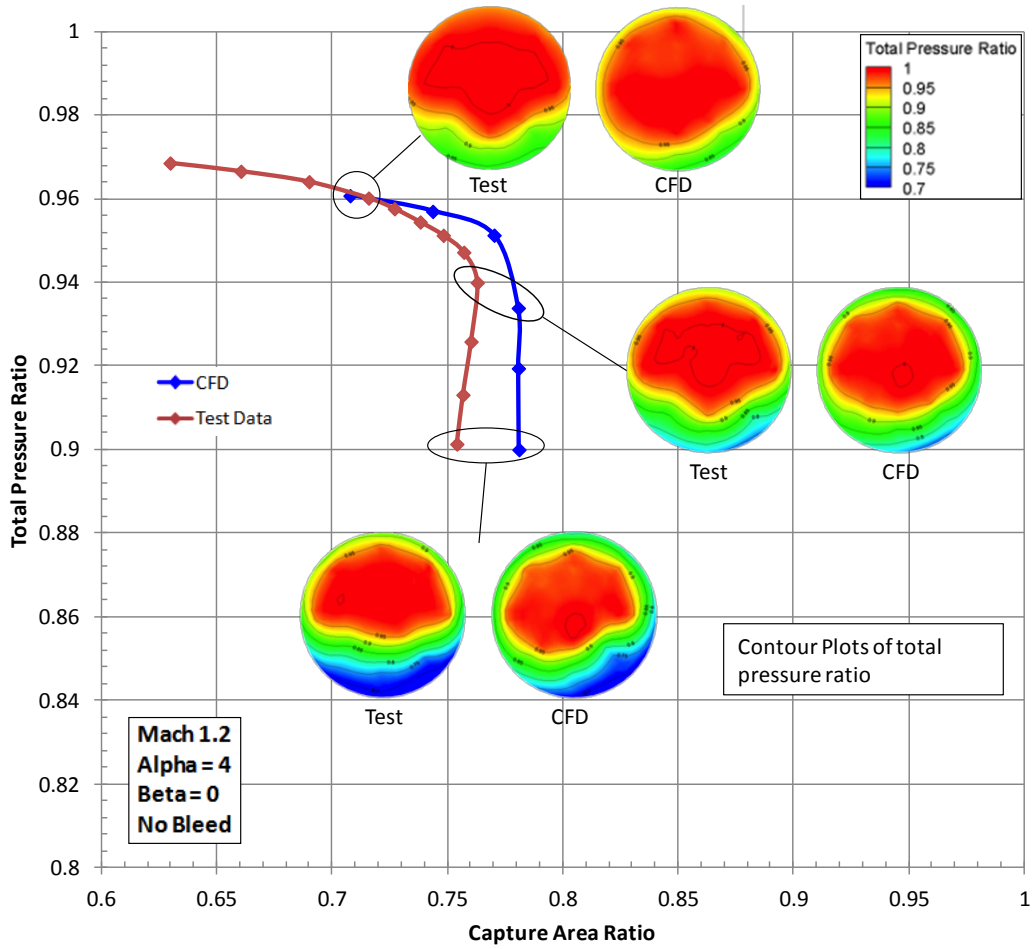

Figure 7-1. Total pressure ratio vs. capture area ratio, Mach 1.2.

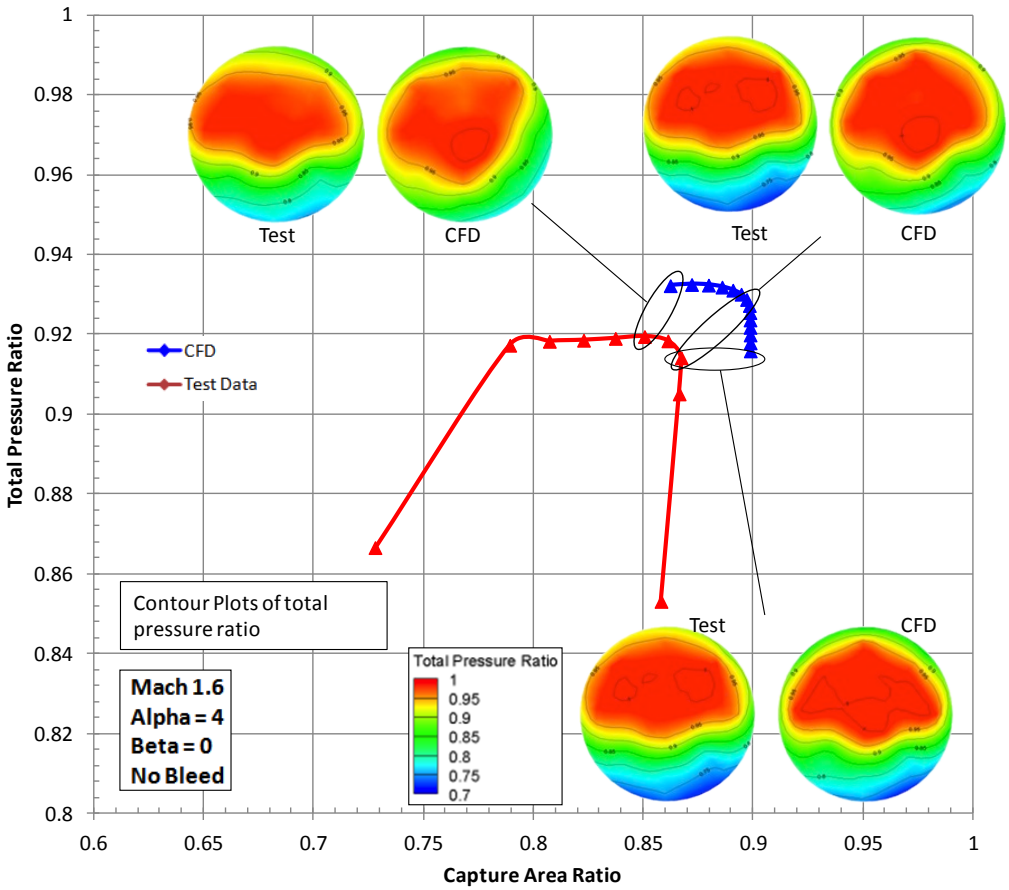

Figure 7-2. Total pressure ratio vs. capture area ratio, Mach 1.6.

In general, CFD results had about the same to 1 percent greater total pressure recovery. CFD tends to underpredict the pressure loss in the subsonic diffuser due to mild separation, and had about 2 percent to 5 percent greater capture area ratio. There is possibility of an issue with the accuracy of the test data air weight flow due to the effect of distortion. This distortion was not present in the mass flow plug calibration test. Plots of total pressure ratio generally agree between the no-bleed test data and CFD, especially at conditions where the pressure recovery is about the same. Even though the no-bleed CFD analysis predicted slightly greater total pressure recovery and slightly lower distortion than the no-bleed test data, test data with the diffuser bleed resulted in significantly greater total pressure recovery and lower distortion than the CFD analysis. The CFD (no-bleed) results were more representative of the test data without bleed than with bleed.

7.2 Sonic Boom Validation

CFD was run to investigate the effect of model configurations on the sonic boom signal and also to provide a basis of comparison to the wind-tunnel pressure rail data. OVERFLOW and CART3D codes were run at the appropriate wind-tunnel conditions. OVERFLOW was run for both viscous and inviscid cases, and comparisons of the results were made. The table below lists the test conditions.

Flow Conditions	Geometry
Mach = 1.6 Re = 4.3e6/ft	Nominal Height above Rail = 62 inches H/L (Performance Model) = ~1.4 H/L (Boom Model) = ~3.9

For a few CFD runs, the geometry was modified to include an estimate of the effect of air loads on the model. This aeroelastic effect was accomplished by twisting the wing −1° in washout, with the twist

varying linearly from root (twist = 0) to the tip (twist $= -1$ degree). For off-track conditions the CFD solutions were extracted at the same location (i.e., a line in space) corresponding to the model and rail orientations in the wind tunnel.

The following figures show some OVERFLOW results for the performance and boom models with variations of angle of attack, roll, and nacelle installations. For these results the model was assumed to be rigid.

Figures 7-3 to 7-7 show the boom model results with N3 nacelles. The three data sets on the charts are representative of the experimental data, the CFD rigid model, and the CFD aeroelastic model. For an angle of attack of 3.1°, the results for roll angles of 0°, 15°, 30°, and 45° are shown. For an angle of attack of 3.6°, only the undertrack results are shown. In general, the boom model experimental data shows some significant rounding or loss of boom signal resolution at these distances from the pressure rail. For the under-track cases in particular, the aeroelastic results tend to match the experimental results better.

Figures 7-8 to 7-11 show the performance model results with the N3 nacelles. The three data sets on the charts are representative of the experimental data, the CFD rigid model, and the CFD aeroelastic model. For an angle of attack of 3.6°, the results for roll angles of 0°, 15°, 30°, and 45° are shown. The performance model experimental results show much better signal resolution at the lower h/l distances to the rail. Features of the peak patterns in the middle of the signal are matched reasonably well. The aeroelastic CFD results show an improvement compared to the rigid results, especially for the under-track case.

Force balance wind-tunnel data results show a significant difference for the N1 to N3 drag increment from predicted increment between N1 and N3 from CFD prediction (13 counts predicted vs. ~45 counts as tested). Some possible explanations for this are the slight changes to the internal duct to accommodate the attachment concept, and the small amount of separation in the duct that was seen during the propulsion test. While the duct geometry change was fairly minor, the flow separation in the duct could be the major contributing factor to the discrepancy.

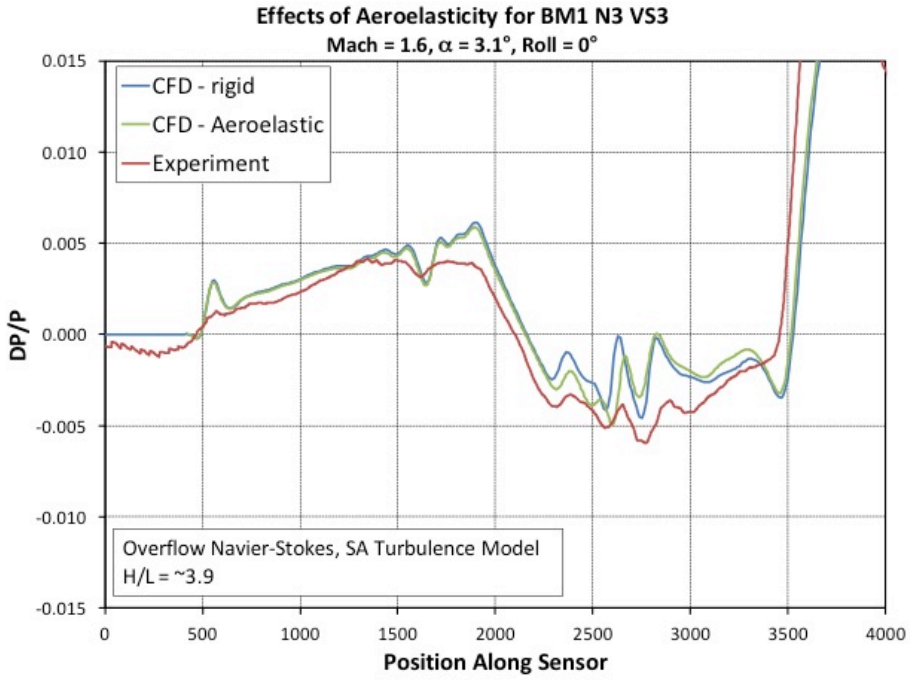

Figure 7-3. Effect of aeroelastics, under-track, 3.1° Alpha, BM model.

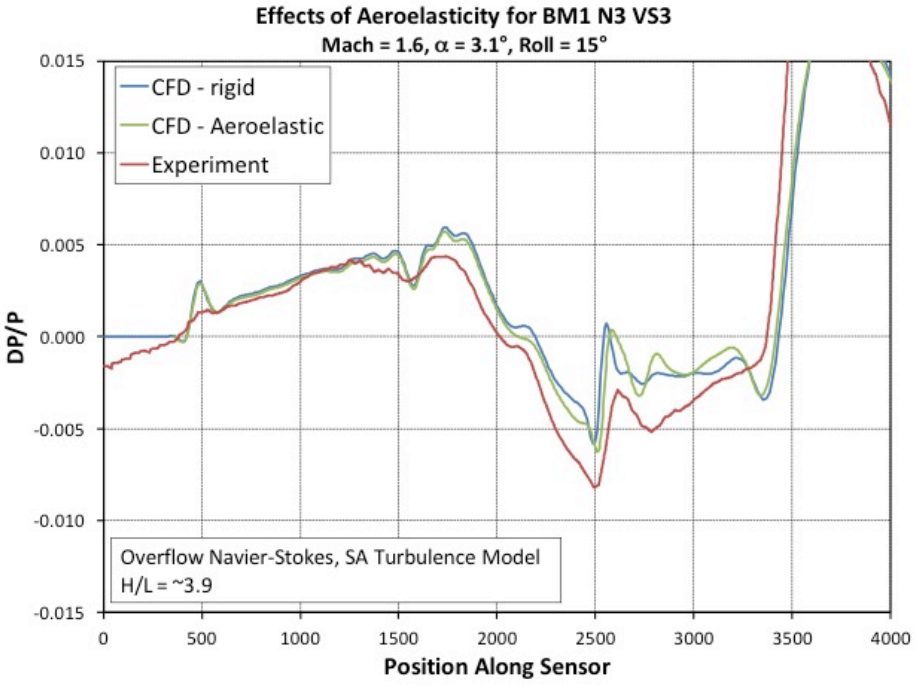

Figure 7-4. Effect of aeroelastics, off-track 15°, 3.1° Alpha, BM model.

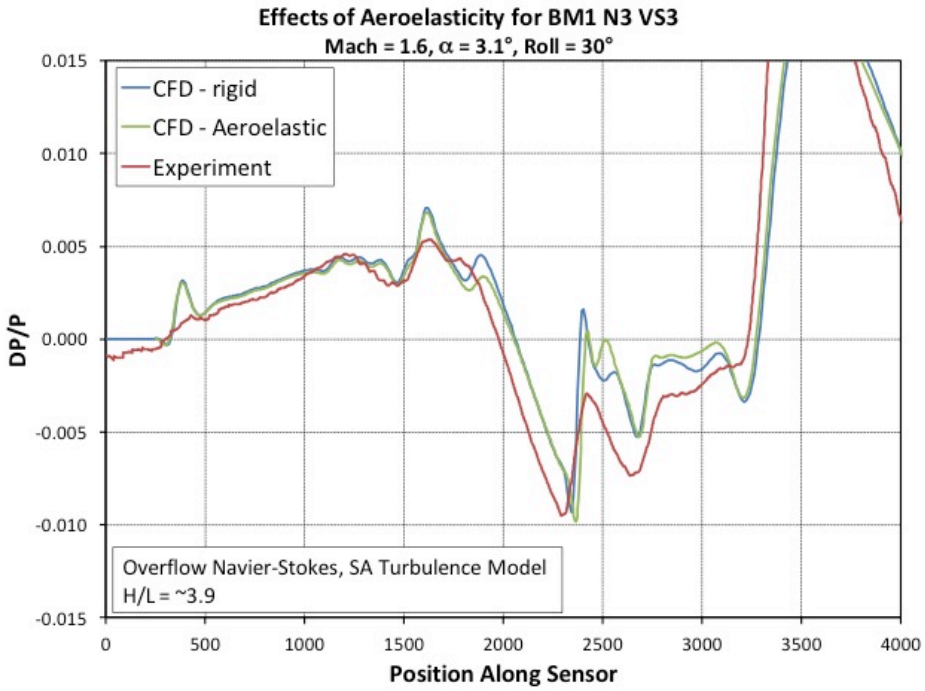

Figure 7-5. Effect of aeroelastics, off-track 30°, 3.1° Alpha, BM model.

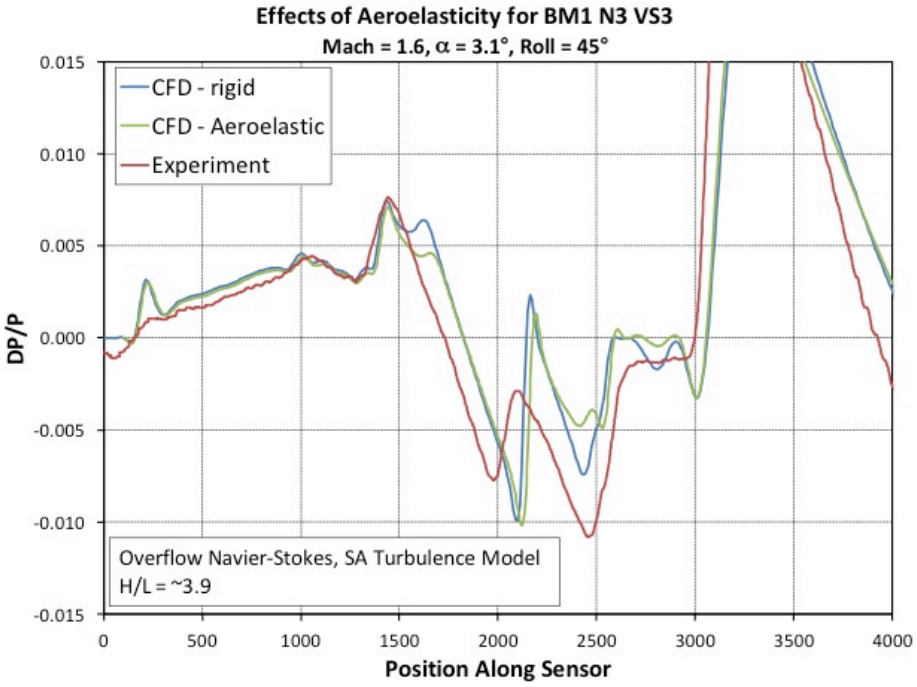

Figure 7-6. Effect of aeroelastics, off-track 45°, 3.1° Alpha, BM model.

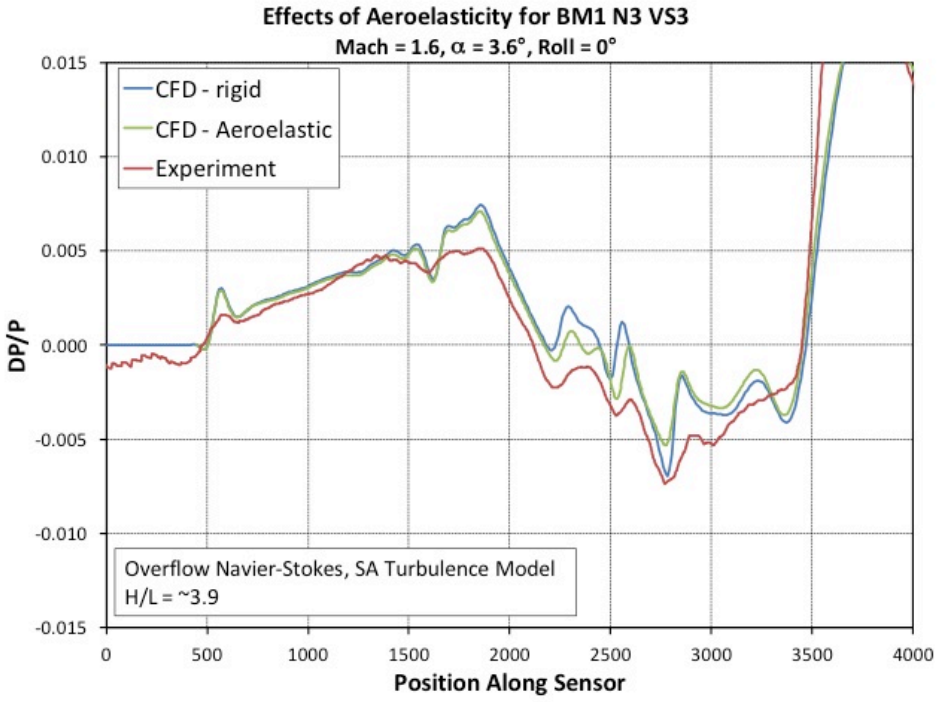

Figure 7-7. Effect of aeroelastics, under-track 3.6°, BM model.

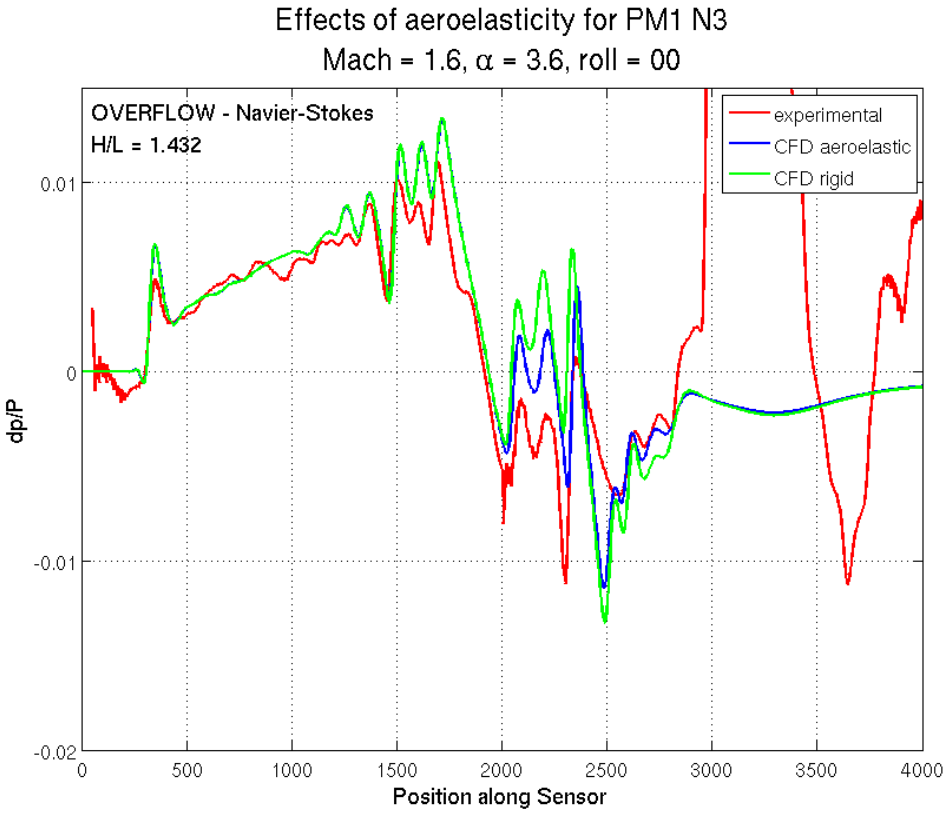

Figure 7-8. Effect of aeroelastics, under-track, 3.6° Alpha, PM model.

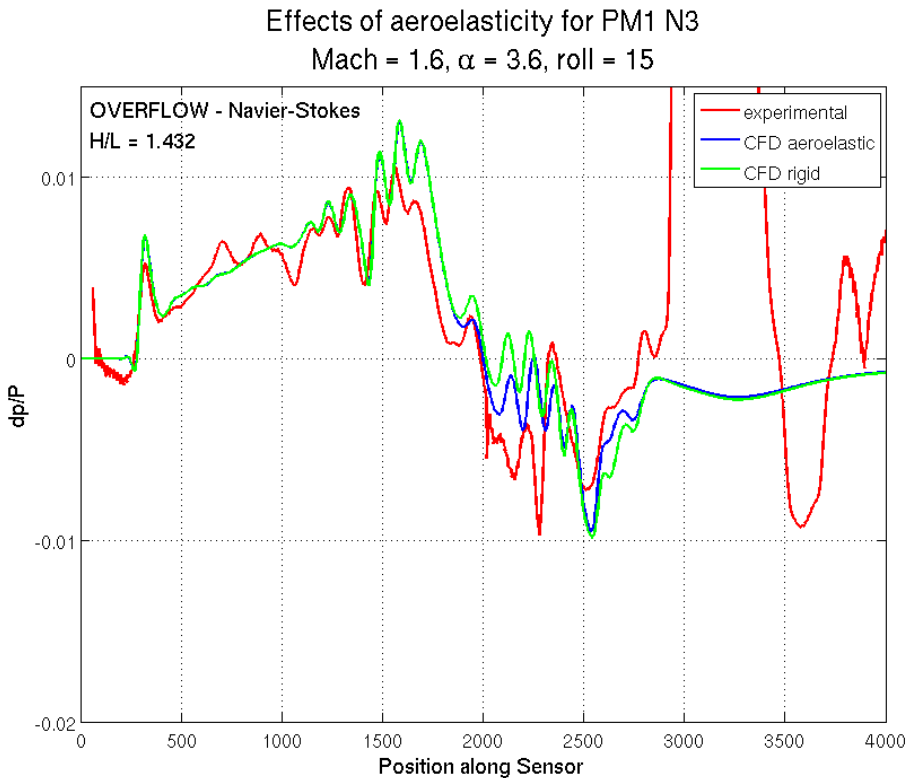

Figure 7-9. Effect of aeroelastics, off-track 15°, 3.6° Alpha, PM model.

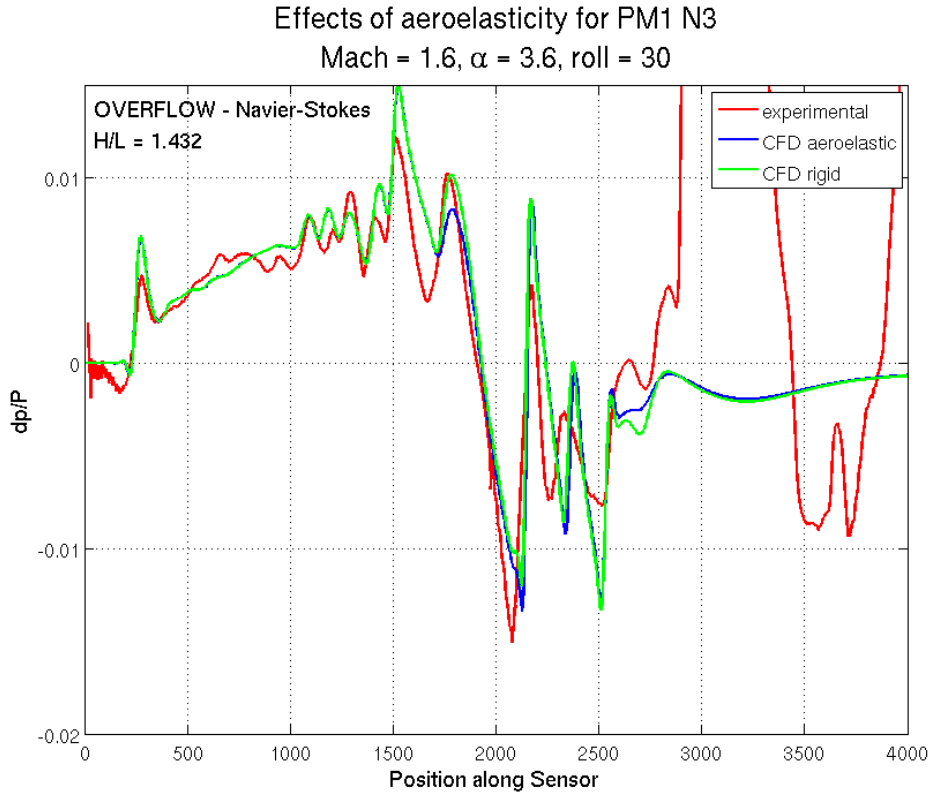

Figure 7-10. Effect of aeroelastics, off-track 30°, 3.6° Alpha, PM model.

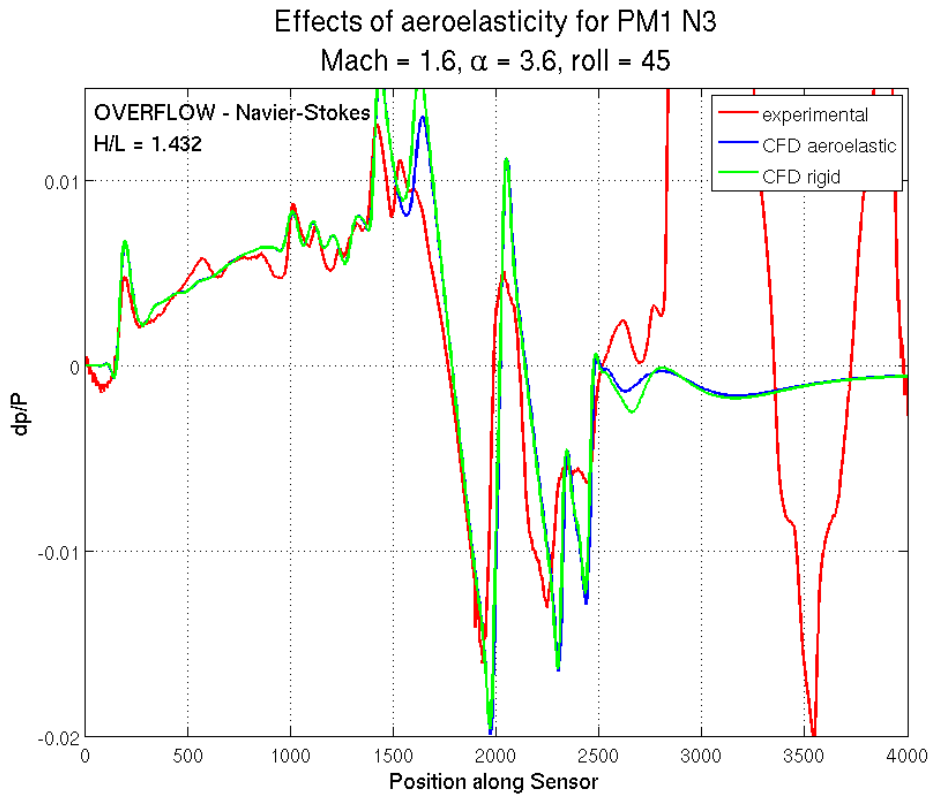

Figure 7-11. Effect of aeroelastics, off-track 45°, 3.6° Alpha, PM model.

7.3 Conclusions

In general, the OVERFLOW code seems to match the experimental data within the measurement uncertainty, particularly for the performance model. The boom model experimental data comparisons are somewhat ambiguous due to the tunnel interferences and data averaging. Some of the mismatches seen in the performance model comparisons could be due to model manufacturing. The CFD results with the estimated aeroelastics show a trend in the correct direction. Force data results from the wind tunnel show a much larger increment for the N3 nacelle. This discrepancy is likely due to internal duct separation and further design or a nacelle calibration could resolve this issue.

8 SUMMARY AND CONCLUSIONS

Summary

Phase II of the N+2 contract continued using the tools and methods selected during Phase I, and further exercised them with a focus on the propulsion integration effects on sonic boom. New overwing inlet concepts were developed to provide acceptable engine performance over a range of conditions. Based on these concepts, new wind tunnel parts were built to test and validate the design methods and CFD codes. The new parts were built to fit the existing Phase I models and included new mounting concepts for the smaller boom model. The wind tunnel testing plan included two short exploratory tests to check the suitability of other NASA facilities that would cover the Mach number range that would be desired for the validation testing. Based on these exploratory tests, and as schedule allowed, the validation testing was split between two facilities – NASA GRC 8 x 6-Foot Wind Tunnel for propulsion testing, and the NASA ARC 9 x 7-Foot Wind Tunnel for force and boom testing.

The propulsion system design effort (inlet and nozzle) utilized design of experiments optimization methods using the OVERFLOW CFD code. Several propulsion and airframe integration concepts were initially evaluated before selecting one for more detailed design work. Both the inlet and nozzle geometries were parametrically varied and the best design was selected based on distortion, recovery, drag, and combined length of the propulsion system. The final designs submitted for testing included a version with an oversized inlet and over-expanded nozzle in order to simulate off design conditions in the wind tunnel. Additionally, a new aft body shape was designed in order to more easily discern engine and plume effect on the boom signal.

New parts for validation wind-tunnel testing were built to be compatible with the existing Phase I models with minor modifications if needed. The following new parts were built for Phase II:

Performance Model:
- Nacelle N3*
- Nacelle N4*
- Contoured Aftbody

*nacelles were segmented so the N3 and N4 inlets and nozzles were interchangeable

Boom Model:
- Nacelle N3
- Nacelle N4
- VS3 Support Strut
- VS4 Support Strut
- VS3/VS4 Compatible body

Propulsion Rig (attached to the Performance Model):
- Nacelle N3 Inlet (no bleed)
- Nacelle N3 Inlet (with bleed)
- Instrumented AIP Section
- Mass Flow Plug Section

The propulsion rig testing was performed at the NASA GRC 8 x 6-Foot Wind Tunnel using two inlets, one without bleed capability and one with four bleed areas – left and right sidewalls, ramp, and diffuser sections. A bleed study was performed in order to identify the best bleed configuration and a matrix of alpha, beta, and Mach number was tested. At each condition, data at approximately 12 plug positions

were taken covering the subcritical through supercritical inlet mass flow range. The results with the selected bleed configuration showed reasonable agreement with pretest recovery predictions. Distortion values were a little higher than expected. However, the KD2 distortion values seem to be reasonable. Inlet performance was acceptable over the typical cruise alpha and beta ranges.

Boom and force testing was performed at the NASA ARC 9 x 7-Foot Wind Tunnel using the 14-inch pressure rail. For the larger performance model, the N3 and N4 nacelles were tested along with the N3 and N4 nozzle/inlet permutations to get a throttle setting effect. Several new parts were fabricated, installed and tested to better discern the plume and aft body close-out effects. These new parts included a tailored "dummy" sting and clamshell parts for the boom and performance models, respectively. Results for the performance model showed reasonable agreement with CFD predictions for both under-track and off-track positions. Wind tunnel drag data was higher for N3 compared to predictions, possibly due to the manufacturing requirements for the nacelle part. For the boom model, two new support systems were used, a mid-body mounted strut (VS3) and a sting mount with a swept strut (VS4). The purpose of VS4 was to provide an aft body shape similar to what was used for the performance model. However, the swept-strut section was too thick and interfered with the boom signal. At the further distances from the rail with the boom models, it was found that the pressure signals showed significant rounding due to tunnel interferences. Results from the VS3 mount were as expected within the data uncertainty measured.

Conclusions

For the propulsion validation test, the objective of demonstrating a feasible inlet was successfully completed. The propulsion rig hardware worked as expected (mechanically) and the test productivity was enhanced by the lessons learned from the exploratory test completed earlier. Inlet bleed was successfully used to improve the inlet performance with a minimal amount of estimated engine performance penalty. Boom validation testing data showed reasonable results for the larger performance model given the amount of data uncertainty. The data showed that the engine integration effects on the boom signal were relatively benign due to the overwing engine installation. Results from the smaller boom model were somewhat ambiguous due to tunnel interferences at the distances tested. Incremental force data for the new nacelle were higher than expected, but the likely cause would be an area of internal duct separation. Since the photogrammetry measured model aeroelastics results were not immediately available after the test, an estimate of the effect was used for the post-test CFD runs. The results from these CFD runs show that, in general, including the estimated aeroelastic effect tended to drive the CFD results closer to the wind-tunnel results. The end result from the validation tests was that inlet/nozzle combination preserved the low-boom characteristics of the QEVC2 configuration while maintaining reasonable inlet and nozzle performance.

Lessons Learned

Design Process

- Viscous analysis is required during the design and optimization phase in order to pick up changes in the inlet flowfield.
- Inlet location drives inlet performance and drag for overwing nacelles. In general, the more forward or inboard the inlet location, results in better recovery and distortion but at the cost of increased drag.

CFD

- Inclusion of the model aeroelastic effects are required for the best agreement with the test data.

- Enhanced grid refinement in the plume shear region provided increased aft signature definition, but did not improve the agreement with the test data. Additional work is needed to determine the ingredients for better test/CFD comparisons.

Testing

- Data quality in the NASA ARC 9 x 7-Foot Wind Tunnel becomes an issue when testing the boom model at further distances from the pressure rail. The NASA GRC 8 x 6-Foot Wind Tunnel showed better results. However, both facilities still require signal averaging.
- The NASA GRC 8 x 6-Foot Wind Tunnel is most productive when testing during the cooler parts of the year in order to minimize disruptions due to a lack of dry air.
- The balance lock-out collars are a very tight fit, and they should be adjusted to a slightly looser fit before being used again.
- The TASK balance does not appear to have issues when used at elevated wind-tunnel temperatures (NASA GRC 8 x 6-Foot Wind Tunnel).
- Bleeding dry air into the NASA ARC 9 x 7-Foot Wind Tunnel test section during offshift hours can significantly reduce the time required to get on condition to the required humidity level.
- The NASA ARC 9 x 7-Foot Wind Tunnel test demonstrated that a single reference run can be used to reduce all data from the test. This is a potential time savings and increase in productivity.
- The NASA ARC 11-Foot Wind Tunnel with the support hardware used has dynamics issues at the higher Mach numbers. Support system damping or changes to the support hardware would need to be done to stabilize the model.
- Productivity for collecting boom data at the NASA GRC 8 x 6-Foot Wind Tunnel is comparable to the NASA ARC 9 x 7-Foot Wind Tunnel if the model is small enough so the linear actuator can be used for positioning.
- Productivity for collecting boom data at the NASA Ames 11-Foot Wind Tunnel is comparable to the NASA ARC 9 x 7-Foot Wind Tunnel.
- Movement of the support system at the NASA GRC 8 x 6-Foot Wind Tunnel has a significant effect on the tunnel flow conditions. Additional time is required to maintain test section Mach number. Alternatively, the linear actuator can be used if the model is small enough.
- A tight Mach tolerance (≤ 0.001) can improve the data quality at the NASA GRC 8 x 6-Foot Wind Tunnel.

9 NOMENCLATURE

Term	Description
2D	Two-Dimensional
3D	Three-Dimensional
765-076E	Boeing N+2 System Study baseline concepts
AIP	Aerodynamic Interface Plane
AOA, Alpha	Angle of Attack
ARC	Ames Research Center
ARRA	American Recovery and Reinvestment Act
AS1, AS2	Body of Revolution AS1, AS2
BCA	Boeing Commercial Airplanes
BETA	Sideslip angle
BM	Boom Model
BOR	Body of Revolution
BR&T	Boeing Research and Technology
CA	Axial Force Coefficient
CART3D	A high-fidelity inviscid analysis package for conceptual and preliminary aerodynamic design
CD	Drag Coefficient
CFD	Computational Fluid Dynamics
CG	Center of Gravity
CL	Lift Coefficient
CM	Pitching Moment Coefficient
CN	Normal Force Coefficient
COTR	Contracting Officer's Technical Representative
Count	1 count of drag is CD = 0.0001
CR	Contractor Report
DOE	Design of Experiments
dP/P	(P-Pinf)/Pinf
ECCI	Elliptical Cowl Cone Inlet
ECRI	Elliptical Cowl Ramp Inlet
FAA	Federal Aviation Administration
FAP	Fundamental Aeronautics Program
FAR	Federal Aviation Regulation
FS	Full Scale

GRC	Glenn Research Center
H	Height
H/L	Height/Length
L/D	Lift/Drag
LaRC	Langley Research Center
LHS	Left-hand side
LMRM	Ames Large Model Roll Mechanism
MDA	Multdisciplinary Analysis
MDBOOM	A Boeing linear wave propagation code
MDO	Multdisciplinary Optimization
MDOPT	A Multidisciplinary Design OPTimization system
MFP	Mass Flow Plug
NASA	National Aeronautics and Space Administration
OML	Outer mold line
OVERFLOW	The OVERset grid FLOW solver. This code solves the Reynolds-Averaged Navier-Stokes equations
PDR	Preliminary Design Review
PLdB	Percieved Loudness in Decibels
QEVC	Quiet Experimental Validation Concept
RHS	Right-hand side
SFC	Specific Fuel Consumption
SMRM	Ames Small Model Roll Mechanism
SSBD	Shaped Sonic Boom Demonstrator
t/c	Thickness to chord ratio
TRANAIR	Nonlinear, full-potential equation code developed to analyze compressible flow over arbitrary complex configurations at subsonic, transonic, or supersonic freestream Mach numbers
USS	Upper Swept Strut
WBS	Work Breakdown Structure

10 REFERENCES

1. Magee, T. E., Wilcox, P. A., Fugal, S. R., Acheson, K. E., Adamson, E. E., Bidwell, A. L., and Shaw, S. G.,"System-Level Experimental Validations for Supersonic Commercial Transport Aircraft Entering Service in the 2018 – 2020 Time Period," NASA /CR-2013-217797, January 2013.
2. Pawlowski, J. W., D. H. Graham, C. H. Boccadoro, P. G. Coen, and D. J. Maglieri, "Origins and Overview of the Shaped Sonic Boom Demonstration Program," AIAA 2005-5-703, 43rd AIAA Aerospace Sciences Meeting and Exhibit, 10–13 January 2005, Reno, Nevada.
3. Norby, W. P., "Small Scale Inlet Testing for Low Cost Screening Applications," AIAA 90-1926, 26th Joint Propulsion Conference, 16-18 July 1990, Orlando, Florida.

REPORT DOCUMENTATION PAGE

Form Approved
OMB No. 0704-0188

1. REPORT DATE *(DD-MM-YYYY)*	2. REPORT TYPE	3. DATES COVERED *(From - To)*
01- 11 - 2015	Contractor Report	

4. TITLE AND SUBTITLE

System-Level Experimental Validations for Supersonic Commercial Transport Aircraft Entering Service in the 2018-2020 Time Period

5a. CONTRACT NUMBER
NNL10AA00T

5b. GRANT NUMBER

5c. PROGRAM ELEMENT NUMBER

6. AUTHOR(S)

Magee, Todd E.; Fugal, Spencer R.; Fink, Lawrence E.; Adamson, Eric E.; Shaw, Stephen G.

5d. PROJECT NUMBER

5e. TASK NUMBER

5f. WORK UNIT NUMBER
475122.02.07.03

7. PERFORMING ORGANIZATION NAME(S) AND ADDRESS(ES)

NASA Langley Research Center
Hampton, Virginia 23681-2199

8. PERFORMING ORGANIZATION REPORT NUMBER

9. SPONSORING/MONITORING AGENCY NAME(S) AND ADDRESS(ES)

National Aeronautics and Space Administration
Washington, DC 20546-0001

10. SPONSOR/MONITOR'S ACRONYM(S)
NASA

11. SPONSOR/MONITOR'S REPORT NUMBER(S)
NASA/CR-2015-218983

12. DISTRIBUTION/AVAILABILITY STATEMENT
Unclassified
Subject Category 02
Availability: NASA STI Program (757) 864-9658

13. SUPPLEMENTARY NOTES
Phase II Final Report

Langley Technical Monitor: Linda S. Bangert

14. ABSTRACT

This report describes the work conducted under NASA funding for the Boeing N+2 Supersonic Experimental Validation project to experimentally validate the conceptual design of a supersonic airliner feasible for entry into service in the 2018 -to 2020 timeframe (NASA N+2 generation). The primary goal of the project was to develop a low-boom configuration optimized for minimum sonic boom signature (65 to 70 PLdB). This was a very aggressive goal that could be achieved only through integrated multidisciplinary optimization tools validated in relevant ground and, later, flight environments. The project was split into two phases. Phase I of the project covered the detailed aerodynamic design of a low boom airliner as well as the wind tunnel tests to validate that design (ref. 1). This report covers Phase II of the project, which continued the design methodology development of Phase I with a focus on the propulsion integration aspects as well as the testing involved to validate those designs.

15. SUBJECT TERMS

Inlet; Sonic boom; Supersonic

16. SECURITY CLASSIFICATION OF:			17. LIMITATION OF ABSTRACT	18. NUMBER OF PAGES	19a. NAME OF RESPONSIBLE PERSON
a. REPORT	b. ABSTRACT	c. THIS PAGE			STI Help Desk (email: help@sti.nasa.gov)
					19b. TELEPHONE NUMBER *(Include area code)*
U	U	U	UU	67	(757) 864-9658